ESO Science Archive Facility - Phase 3 Data Release Description
ESO public survey programme UltraVISTA - Ultra Deep Survey with VISTA, Data Release DR4.1
provided by J.S. Dunlop, submitted between 2022-04-13 and 2022-06-21, published on 2022-06-30
release description document revised on 2022-06-30

The COSMOS2020 catalogue

J. R. Weaver, O. B. Kauffmann, O. Ilbert, H. J. McCracken, A. Moneti, S. Toft, G. Brammer, M. Shuntov, I. Davidzon, B. C. Hsieh, C. Laigle, A. Anastasiou, C. K. Jespersen, J. Vinther, P. Capak, C. M. Casey, C. J. R. McPartland, B. Milvang-Jensen, B. Mobasher, D. B. Sanders, L. Zalesky, S. Arnouts, H. Aussel, J. S. Dunlop, A. Faisst, M. Franx, L. J. Furtak, J. P. U. Fynbo, K. M. L. Gould, T. R. Greve, S. Gwyn, J. S. Kartaltepe, D. Kashino, A. M. Koekemoer, V. Kokorev, O. Le Fèvre, S. Lilly, D. Masters, G. Magdis, V. Mehta, Y. Peng, D. A. Riechers, M. Salvato, M. Sawicki, C. Scarlata, N. Scoville, R. Shirley, J. Silverman, A. Sneppen, V. Smolčić, C. Steinhardt, D. Stern, M. Tanaka, Y. Taniguchi, H. I. Teplitz, M. Vaccari, W.-H. Wang, G. Zamorani

June 29, 2022

Data Collection:	`UltraVISTA`
Release number	`4.1`
Data provider:	`John Weaver, Bo Milvang-Jensen, Jim Dunlop`
Date:	`June 29, 2022`

1 Abstract

This document describes the COSMOS2020 catalogues which are distributed through ESO's Phase 3 (in the UltraVISTA Phase 3 collection under the label DR4.1). In these catalogues, source detection and multi-wavelength photometry is performed for 1.7 million sources in the 2 deg^2 COSMOS field. Approximately 966 000 of these sources are measured with all available broad-band data using both traditional aperture photometry and a new profile-fitting photometric tool, The Farmer, which we have developed. Photometric redshifts are computed for all sources in each catalogue using two independent photometric redshift codes, `LePhare` and `EAZY`. At $i < 21$, sources have sub-percent photometric redshift precision and even the faintest sources at $25 < i < 27$ reach a photometric redshift accuracy of 5 %.

1.1 Acknowledging these data products

If you use these catalogues, please cite the following paper: "COSMOS2020: A panchromatic view of the Universe to $z \sim 10$ from two complementary catalogues", Weaver et al. (2022). You must also include the following standard acknowledgement:

"Based on observations collected at the European Southern Observatory under ESO programme ID 179.A-2005 and on data products produced by CALET and the Cambridge Astronomy Survey Unit on behalf of the UltraVISTA consortium."

If the access to the ESO Science Archive Facility services was helpful for you research, please include the following acknowledgement: "This research has made use of the services of the ESO Science Archive Facility."

You are additionally encouraged to cite the papers describing the data sets included in the catalogue (such as McCracken et al. 2012 for UltraVISTA).

2 Changes with respect to previous versions

2.1 Changes from COSMOS2015 to COSMOS2020

The previous COSMOS catalogue was COSMOS2015 (Laigle et al. 2016). It was released in Phase 3 under the label UltraVISTA DR2.1, as the catalogue was based on the UltraVISTA DR2 imaging. It was the first COSMOS catalogue to be released via Phase 3. COSMOS2015 consisted of a single catalogue. COSMOS2020 (Weaver et al. 2022), which is the subject of this document, consists of two catalogues, called Classic and The Farmer (see Sect. 3.2). COSMOS2020 is based on the UltraVISTA DR4 imaging, and is released in Phase 3 under the label UltraVISTA DR4.1.

2.2 Changes from the initial public version of COSMOS2020 to the Phase 3 version

The COSMOS2020 catalogues and supporting files were initially made publicly available on our website `https://cosmos2020.calet.org/` when the Weaver et al. paper appeared on arXiv on 28 Oct 2021 (`https://arxiv.org/abs/2110.13923`). We subsequently made an updated version, as described in Sect. 2.2.1 and 2.2.2 below. This version is released via Phase 3, and has since 24 Jun 2022 also been made available on our website, replacing the initial version.

2.2.1 Bug fixes and minor improvements

Many of the following changes were not directly due to Phase 3 requirements, but were often a result of our work preparing the Phase 3 release, and some of the bugs were discovered by ESO's Phase 3 scientist Laura Mascetti.

- Classic: negative values in the column `FLUX_RADIUS` were set to NaN
- The Farmer: corrected the column names for the four `ACS_F814W` columns (which lacked the `ACS_` part)
- The Farmer: added columns `MODEL_FLAG` and `GROUP_ID`, and removed column `VALID_SOURCE` (which was not needed after the introduction of column `MODEL_FLAG`)
- The Farmer: set all column values to NULL for sources that moved more than $0.6''$ from their detection position (these sources can be identified by the `MODEL_FLAG` column being set to 2)
- The Farmer: column `SOLUTION_MODEL` was empty, now fixed
- Classic and The Farmer: added the `ez_ssfr` column
- Classic and The Farmer: the value of the `TNULL` keywords were changed from two incorrect values to the intended value of -99
- Classic and The Farmer: the column `lp_age` was missing a unit (`TUNIT`), now fixed

- CLASSIC and THE FARMER: The catalogues contain the columns `ez_mass` (log stellar mass), `ez_sfr` (log SFR), and `ez_Lv` (log V-band luminosity). For each of these physical quantities the catalogues also contain five percentile columns, e.g. `ez_mass_p025` for the 2.5% percentile. Before the change, the values in these 3×5 percentile columns corresponded to the linear version of the quantity, while after the change they correspond to the logarithmic version

- CLASSIC and THE FARMER: the columns `lp_age`, `lp_dust`, `lp_mass_best`, `lp_SFR_best` and `lp_sSFR_best` used -99.9 to indicate NULL, which was changed to NaN

- CLASSIC: the columns `SPLASH_CH1_MAG`, `SPLASH_CH2_MAG`, `SPLASH_CH3_MAG`, `SPLASH_CH4_MAG`, `SPLASH_CH1_MAGERR`, `SPLASH_CH2_MAGERR`, `SPLASH_CH3_MAGERR` and `SPLASH_CH4_MAGERR` used -99.9 to indicate NULL, which was changed to NaN

2.2.2 Changes directly related to the Phase 3 requirements

All of the following changes relate only to the header part of the FITS files, not to the data part. These changes were made so that the data products meet the requirements defined in the ESO Science Data Products Standard document, available from the Phase 3 website[1].

- The required metadata were added to the primary headers. This includes metadata relevant to the ESO data only (here the UltraVISTA DR4 imaging in the 5 bands), such as provenance, time span, ESO programme IDs, filter names and limiting magnitudes, and metadata relevant to the catalogue as a whole, such as the footprint on the sky and the bibcode for the paper to be referenced

- For each of the almost 1200 columns in the two catalogues we wrote a description of length up to 68 characters; these descriptions are probably quite useful to the typical user. The descriptions are found in the extension 1 FITS headers (in the `TCOMM` keywords) and are listed in this document in Appendix 6.1 and 6.2

- For each column we also wrote a Unified Content Descriptor Version 1+ (UCD1+)[2]. This is a standardised vocabulary. An example could be `stat.error;phot.mag;em.opt.R` which means a statistical error on a photometric magnitude for electromagnetic radiation between 600 and 750 nm. Writing the UCDs was a substantial and complex task, and we acknowledge discussions with ESO and the IVOA Semantics group. These UCDs are found in the extension 1 header (in the `TUCD` keywords), but not given here in this document

- The extension 1 headers already contained units (in the `TUNIT` keywords), but expressed in the format/syntax of the `astropy` package (Robitaille et al. 2013; Astropy Collaboration et al. 2018). The units were changed to follow the ESO standard (see Sect. 8 of the ESO Data Interface Control Document[3]), which implements a subset of the IVOA standard[4]. The updated units are in the `TUNIT` keywords and are also listed in Appendix 6.1 and 6.2.

[1] `https://www.eso.org/sci/observing/phase3.html`
[2] `https://www.ivoa.net/documents/UCD1+/`
[3] `https://archive.eso.org/cms/tools-documentation/eso-data-interface-control.html`
[4] `https://ivoa.net/documents/VOUnits/`

Examples of changes:
`pix2` → `pix**2`
`dex(solLum)` → `log(solLum)`
`solLum-1 solMass` → `solMass/solLum`

We verified the correctness of the UCDs and units using STILTS (Taylor 2006), using votlint[5] and the VO-tools[6] (based on ucidy[7] and unity[8]), and the overall Phase 3 verification was performed by ESO. The files with the updates described in this and the previous subsections were named `R1_v2.1_p3` and are released via this ESO Phase 3 release. (See the note on filenames in Sect. 4.)

3 Release notes

In the following Sections, a highly condensed description of both catalogues is presented. For full details, see Weaver et al. (2022).

3.1 COSMOS2020 imaging data

The principal improvements in COSMOS2020 compared to previous COSMOS catalogues and the previous ESO Phase 3 COSMOS catalogue are the significantly deeper optical and near-infrared images from ongoing Subaru-HSC and VISTA-VIRCAM surveys. In addition, this release contains the definitive reprocessing of all Spitzer data ever taken on COSMOS. 'Legacy' or pre-existing data sets present in the previous COSMOS2015 catalogue have been reprocessed to take advantage of improved astrometry from Gaia (the only exceptions being external ancillary data such as GALEX). All images are resampled to final stacks with a $0''.15$ pixel scale. These stacks are aligned to the COSMOS tangent point, which has a right ascension and declination (J2000) of (10h00m27.92s $+02°12'03''.50$). For full details, see Weaver et al. (2022).

3.2 Photometric measurements

For the new COSMOS2020 catalogues, two independent photometric catalogues are computed using two different techniques. In both cases, the input source list is made by detecting objects on a deep $izJYHK_{\rm s}$ combined `CHI-MEAN` image (defined in Appendix B of Drlica-Wagner et al. 2018) generated using `SWarp`. This image is optimised for the detection of high-redshift objects.

One catalogue is generated using the same photometric measurement methods as our previous COSMOS2015 catalogue (Laigle et al. 2016). Objects are detected with `SExtractor` (Bertin & Arnouts 1996) and for each galaxy, colours are computed using using aperture photometry performed on PSF-homogenized images (except for Spitzer/IRAC bands, where PSF-fitting with the `IRACLEAN` software (Hsieh et al. 2012) is used). This is called the "Classic" catalogue.

[5] `http://www.star.bristol.ac.uk/~mbt/stilts/sun256/votlint.html`
[6] `http://www.star.bristol.ac.uk/~mbt/stilts/sun256/uk.ac.starlink.ttools.func.VO.html`
[7] `https://github.com/gmantele/ucidy`
[8] `https://code.nxg.name/nxg/unity`

The second photometric catalogue is created using the `The Tractor` (Lang et al. 2016) package starting from a slightly different source list derived independently with `SEP` Barbary (2016) (a `python` implementation of `SExtractor`). `The Tractor` derives parametric models from one or more images containing morphological information. An associated package, The Farmer (Weaver et al., in prep.), generates a full multi-wavelength catalogue using `The Tractor` to perform the modelling. This approach has the advantage that `The Tractor` does not require a high-resolution image and can hence be consistently applied to ground-based data sets (and no PSF homogenization is required). Because the models are purely parametric, `The Tractor` can provide basic shape measurements for resolved sources in addition to fluxes. Detailed comparisons of both photometric catalogues and the quality of the derived photo-z are presented in Weaver et al. (2022).

Both catalogues have their advantages and disadvantages, and the choice of which catalogue to use should be made based on the scientific application in question. Having multiple photometric redshifts for a large subset of sources can also be invaluable for validation and testing of specific measurements in COSMOS.

3.3 Photometric redshifts and physical parameters

Photometric redshifts and physical parameters are computed for both catalogues using `LePhare` (Arnouts et al. 2002; Ilbert et al. 2006) and `EAZY` (Brammer et al. 2008). Results from both packages are broadly in agreement, but once again, the choice of which package to use must be made based on the scientific application in question.

3.4 Astrometric calibration

Astrometric solutions were computed for all optical, infrared and near-infrared data using the Gaia references catalogues (DR1 or DR2; Gaia Collaboration et al. (2016, 2018)). In general, the agreement between positions of sources in each of the stacks with the external references catalogues and between sources in different bands is around 10 mas and 1 mas respectively.

4 Release Content

Table 1 lists the data products (files) in this release. Note that throughout this document, the file names are the ones we have used in our upload to the ESO Phase 3 system. Upon publication in the Phase 3 system / ESO Science Archive Facility, the files are renamed `ADP` followed by a publication timestamp. As an example, the COSMOS2015 catalogue is called `ADP.2016-12-15T11:49:34.984.fits`. ADP means Advanced Data Products. The original file name is recorded in the keyword `ORIGFILE` in the primary header. Table 2 lists the correspondence between the ADP IDs and the original filenames.

One of our data products is a tar file, containing a mix of relevant files: mask files in the form of ds9 region files, and two Python code fragments. The files in the tar file are listed in Table 3. A full description of the masks is provided in Section 4.6.

Table 1: Data products delivered with this release

Filename	Description
COSMOS2020_CLASSIC_R1_v2.1_p3.fits	CLASSIC catalogue, see Section 4.2.
COSMOS2020_CLASSIC_R1_v2.1_LEPHARE_PZ_p3.fits	Redshift probability distributions, see Section 4.7.
COSMOS2020_CLASSIC_R1_v2.1_EAZY_CZ_p3.fits	Redshift probability distributions, see Section 4.7.
COSMOS2020_FARMER_R1_v2.1_p3.fits	THE FARMER catalogue, see Section 4.4.
COSMOS2020_FARMER_R1_v2.1_LEPHARE_PZ_p3.fits	Redshift probability distributions, see Section 4.7.
COSMOS2020_FARMER_R1_v2.1_EAZY_CZ_p3.fits	Redshift probability distributions, see Section 4.7.
COSMOS2020_izYJHKs_chimean-v3_p3.fits	CHI_MEAN detection image.
COSMOS2020_extra_p3.tar	Supplementary files, see Table 3.

Table 2: Correspondence between original filenames and ADP IDs

Filename	ADP ID
COSMOS2020_CLASSIC_R1_v2.1_p3.fits	ADP.2022-06-21T19:13:38.107
COSMOS2020_CLASSIC_R1_v2.1_LEPHARE_PZ_p3.fits	ADP.2022-06-21T19:13:38.108
COSMOS2020_CLASSIC_R1_v2.1_EAZY_CZ_p3.fits	ADP.2022-06-21T19:13:38.109
COSMOS2020_FARMER_R1_v2.1_p3.fits	ADP.2022-06-21T19:13:38.112
COSMOS2020_FARMER_R1_v2.1_LEPHARE_PZ_p3.fits	ADP.2022-06-21T19:13:38.113
COSMOS2020_FARMER_R1_v2.1_EAZY_CZ_p3.fits	ADP.2022-06-21T19:13:38.114
COSMOS2020_izYJHKs_chimean-v3_p3.fits	ADP.2022-06-21T19:13:38.110
COSMOS2020_extra_p3.tar	ADP.2022-06-21T19:13:38.111

4.1 Labels used for the various photometric datasets

The two COSMOS2020 catalogues contain photometry based on a number of datasets. For each of the 44 datasets we have assigned a label given in Table 4; this label is used in the column names (see the complete lists of columns names in Sections 6.1 and 6.2). Note that for most datasets we performed the photometry ourselves (Weaver et al. 2022), while for GALEX, ACS and SPLASH the photometry was crossmatched from external catalogues (see our README files in Sections 4.3 and 4.5).

Table 3: Contents of the tar file

Filename	Description
MASK_SUPCAM_COSMOS2020.reg	Suprime-cam mask file.
MASK_HSC-stars_griz_COSMOS2020.reg	HSC mask file.
MASK_UDEEP_COSMOS2020.reg	Mask file for the Ultra-Deep regions.
MASK_UVISTA_COSMOS2020.reg	Mask file for the UltraVISTA area.
MASKS_README.txt	Description of the masks.
flags_in_catalog.png	Mask illustration (Figure 1).
eazy_zcdf_pdf.txt	Code fragment to compute photo-z PDFs from EAZY output.
COSMOS2020_prepare_apertures.txt	Code fragment to compute photometry from CLASSIC catalogue.

Table 4: The photometric datasets

Label	Description	$\lambda_{\rm central}$ [Å]	width[Å]
GALEX_FUV	GALEX FUV	1526	224
GALEX_NUV	GALEX NUV	2307	791
CFHT_u	CFHT/MegaCam u	3709	518
CFHT_ustar	CFHT/MegaCam u*	3858	598
ACS_F814W	HST/ACS F814W	8333	2511
HSC_g	Subaru/HSC HSC-SSP PDR2 g	4847	1383
HSC_r	Subaru/HSC HSC-SSP PDR2 r	6219	1547
HSC_i	Subaru/HSC HSC-SSP PDR2 i	7699	1471
HSC_z	Subaru/HSC HSC-SSP PDR2 z	8894	766
HSC_y	Subaru/HSC HSC-SSP PDR2 y	9761	786
SC_B	Subaru/SuprimeCam B	4488	892
SC_gp	Subaru/SuprimeCam g+	4804	1265
SC_V	Subaru/SuprimeCam V	5487	954
SC_rp	Subaru/SuprimeCam r+	6305	1376
SC_ip	Subaru/SuprimeCam i+	7693	1497
SC_zp	Subaru/SuprimeCam z+	8978	847
SC_zpp	Subaru/SuprimeCam z++	9063	1335
SC_IB427	Subaru/SuprimeCam IB427	4266	207
SC_IB464	Subaru/SuprimeCam IB464	4635	218
SC_IA484	Subaru/SuprimeCam IA484	4851	229
SC_IB505	Subaru/SuprimeCam IB505	5064	231
SC_IA527	Subaru/SuprimeCam IA527	5261	243
SC_IB574	Subaru/SuprimeCam IB574	5766	273
SC_IA624	Subaru/SuprimeCam IA624	6232	300
SC_IA679	Subaru/SuprimeCam IA679	6780	336
SC_IB709	Subaru/SuprimeCam IB709	7073	316
SC_IA738	Subaru/SuprimeCam IA738	7361	324
SC_IA767	Subaru/SuprimeCam IA767	7694	365
SC_IB827	Subaru/SuprimeCam IB827	8243	343
SC_NB711	Subaru/SuprimeCam NB711	7121	72
SC_NB816	Subaru/SuprimeCam NB816	8150	120
UVISTA_Y	VISTA/VIRCAM UltraVISTA DR4 Y	10216	923
UVISTA_J	VISTA/VIRCAM UltraVISTA DR4 J	12525	1718
UVISTA_H	VISTA/VIRCAM UltraVISTA DR4 H	16466	2905
UVISTA_Ks	VISTA/VIRCAM UltraVISTA DR4 Ks	21557	3074
UVISTA_NB118	VISTA/VIRCAM UltraVISTA DR4 NB118	11909	112
IRAC_CH1	Spitzer/IRAC ch1	35686	7443
IRAC_CH2	Spitzer/IRAC ch2	45067	10119
IRAC_CH3	Spitzer/IRAC ch3	57788	14082
IRAC_CH4	Spitzer/IRAC ch4	79958	28796
SPLASH_CH1	Spitzer/IRAC SPLASH ch1	35686	7443
SPLASH_CH2	Spitzer/IRAC SPLASH ch2	45067	10119
SPLASH_CH3	Spitzer/IRAC SPLASH ch3	57788	14082
SPLASH_CH4	Spitzer/IRAC SPLASH ch4	79958	28796

Note: see also Table 1 in Weaver et al. (2022).

4.2 The Classic catalogue

The Classic catalogue contains 754 columns and 1,720,700 rows. We provide positional matches with ACS, X-Ray, UV, and also with previous COSMOS catalogues including COSMOS2015. Note that the FIR and radio matches are not provided as a consistent photometry of these often confusion-limited sources will be done in future work following. Sect. 4.3 provides the README file distributed with the catalogue describing each column. Additionally, in Sect. 6.1 we list all the 754 columns together with their number name and description. Note that the Classic catalogue covers a larger area than the The Farmer area, which covers only the UltraVISTA area; this is why there are more sources present in that catalogue.

4.3 Description of Classic catalogue columns

```
The CLASSIC COSMOS2020 photometric catalog

We present here the catalog containing the photometry extracted with
SExtractor and IRACLEAN, for about 1,700,000 sources in the COSMOS
field. The photometry from optical/NIR was extracted from
PSF-homogenized images, with a target PSF set to a Moffat profile with
parameters (0.8",2.5).  The full description of this catalog is in
Weaver et al., 2022a (ApJS 258 11)

Updated 02/2022
Contact: john.weaver.astro@gmail.com


#########################################################
Identification
#########################################################

Identifier
#   name = 'ID'

Right Ascension and Declination
#   name = 'ALPHA_J2000'; unit = 'deg'
#   name = 'DELTA_J2000'; unit = 'deg'

Position
#   name = 'X_IMAGE'; unit = 'pixel'
#   name = 'Y_IMAGE'; unit = 'pixel'
#   name = 'ERRX2_IMAGE'; unit = 'pixel'
#   name = 'ERRY2_IMAGE'; unit = 'pixel'
#   name = 'ERRXY_IMAGE'; unit = 'pixel'

Radius of circle enclosing 50% of total flux from the PSF-homogenized Ks band image
#   name = 'FLUX_RADIUS'; unit = 'pixel'
Reduced pseudo-radius derived from the izYJHKs area of the detection image
#   name = 'KRON_RADIUS'; unit = 'unitless'

#########################################################
Flags
#########################################################

Flags are computed from the region files included with the release

Flag for the bright stars and edges of the HSC images
#   name = 'FLAG_HSC'      (0:clean, 1:masked)

Flag for the bright stars and edges of the Suprime-Cam images
#   name = 'FLAG_SUPCAM'   (0:clean, 1:masked)
```

```
Flag for the UltraVISTA region
#   name = 'FLAG_UVISTA'   (0:inside, 1:outside)

Flag for the UltraVISTA ultra-deep regions
#   name = 'FLAG_UDEEP'    (0:ultra-deep, 1:deep)

Flag for the combination of FLAG_UVISTA, FLAG_HSC and FLAG_SUPCAM
#   name = 'FLAG_COMBINED' (0:clean and inside UVISTA)

#########################################################
Galactic extinction at the object position
#########################################################

E(B-V) values from Schlegel, Finkbeiner & Davis (1998) dust map
By default, a scaling of 0.86 is applied to the map values
to reflect the recalibration by Schlafly & Finkbeiner (2011)

#   name = 'EBV_MW'; unit = 'mag'

#########################################################
Photometry
#########################################################

No data convention
flux, fluxerr, mag, magerr = NaN

Negative flux convention
mag, magerr = NaN

NOTE: The photometry is not corrected for Milky Way extinction.
NOTE: The photometry is not corrected for photometric offsets derived
by LePhare or EAZY
NOTE: The aperture photometry errors are corrected
for the correlated noise in the images.

#########################################################

List of bands
CFHT/MegaCam (CLAUDS):
  CFHT_ustar, CFHT_u
Subaru/Hyper Suprime-Cam (HSC SSP DR2):
  HSC_g, HSC_r, HSC_i, HSC_z, HSC_y
VISTA/VIRCAM (UltraVISTA DR4):
  UVISTA_Y, UVISTA_J, UVISTA_H, UVISTA_Ks, UVISTA_NB118
Subaru/Suprime-Cam:
  SC_IB427, SC_IB464, SC_IA484, SC_IB505, SC_IA527, SC_IB574, SC_IA624,
  SC_IA679, SC_IB709, SC_IA738, SC_IA767, SC_IB827, SC_NB711, SC_NB816,
  SC_B, SC_gp, SC_V, SC_rp, SC_ip, SC_zp, SC_zpp

NOTE: SC_gp is not used for photo-z. See paper for details.

2" diameter aperture fluxes, flux errors, magnitudes and magnitude errors
#   name = '###_FLUX_APER2';    unit = 'uJy'
#   name = '###_FLUXERR_APER2'; unit = 'uJy'
#   name = '###_MAG_APER2';    unit = 'mag'
#   name = '###_MAGERR_APER2'; unit = 'mag'

3" diameter aperture fluxes, flux errors, magnitudes and magnitude errors
#   name = '###_FLUX_APER3';    unit = 'uJy'
#   name = '###_FLUXERR_APER3'; unit = 'uJy'
#   name = '###_MAG_APER3';    unit = 'mag'
#   name = '###_MAGERR_APER3'; unit = 'mag'

Kron aperture fluxes, flux errors, magnitudes and magnitude errors
```

```
#   name = '###_FLUX_AUTO';    unit = 'uJy'
#   name = '###_FLUXERR_AUTO'; unit = 'uJy'
#   name = '###_MAG_AUTO';    unit = 'mag'
#   name = '###_MAGERR_AUTO'; unit = 'mag'

Isophotal magnitudes and magnitude errors
#   name = '###_MAG_ISO';    unit = 'mag'
#   name = '###_MAGERR_ISO'; unit = 'mag'

#########################################################

Internal flags from SExtractor, combined into a single number by
adding the values (1, 2, 4, ...) for the flags listed below:

#  name = '###_FLAGS'

 1  The object has neighbours, bright and close enough to significantly bias the
     MAG_AUTO photometry, or bad pixels (more than 10% of the integrated area affected),
 2  The object was originally blended with another one,
 4  At least one pixel of the object is saturated (or very close to),
 8  The object is truncated (too close to an image boundary),
 16 Object's aperture data are incomplete or corrupted,
 32 Object's isophotal data are incomplete or corrupted,
 64 A memory overflow occurred during deblending,
 128 A memory overflow occurred during extraction.

External flag from SExtractor, with the used external flag image being
one having a value of 4 for saturated pixels and 0 otherwise, so this
column will have a value of 4 if there were saturated pixel(s) in the
isophotal area of the object


#  name = '###_IMAFLAGS_ISO

#########################################################

Aperture-to-total magnitude corrections for 2" and 3" diameter
aperture photometry, respectively. To be added to ###_MAG_APER# to get
total magnitudes


#   name = 'total_off2'; unit = 'mag'
#   name = 'total_off3'; unit = 'mag'

#########################################################

List of bands
Spitzer/IRAC (Cosmic DAWN Survey):
  IRAC_CH1, IRAC_CH2

IRACLEAN fluxes, flux errors, magnitudes and magnitude errors
#   name = '###_FLUX';    unit = 'uJy'
#   name = '###_FLUXERR'; unit = 'uJy'
#   name = '###_MAG';    unit = 'mag'
#   name = '###_MAGERR'; unit = 'mag'

NOTE: IRACLEAN photometry of IRAC_CH3 and IRAC_CH4 are not extracted
with IRACLEAN

#####################################################
Ancillary photometry

NOTE: All are matched within 0.6" radius
#####################################################
```

```
GALEX photometry (Zamojski et al. 2007) from the Capak et al. 2007
catalog

Matched identifier
#   name = 'ID_GALEX'

List of bands
  GALEX_NUV, GALEX_FUV

#   name = '###_FLUX';    unit = 'uJy'
#   name = '###_FLUXERR'; unit = 'uJy'
#   name = '###_MAG';    unit = 'mag'
#   name = '###_MAGERR'; unit = 'mag'

#####################################################

SPLASH photometry from the COSMOS2015 catalog (Laigle et al. 2016)

Matched identifier
#   name = 'ID_COSMOS2015'

List of bands
  SPLASH_CH1, SPLASH_CH2, SPLASH_CH3, SPLASH_CH4

#   name = '###_FLUX';    unit = 'uJy'
#   name = '###_FLUXERR'; unit = 'uJy'
#   name = '###_MAG';    unit = 'mag'
#   name = '###_MAGERR'; unit = 'mag'

#####################################################

HST/ACS catalog (Leauthaud et al. 2007)
selection: CLEAN == 1

Matched identifier
#   name = 'ID_ACS'

ACS photometry
#   name = 'ACS_F814W_FLUX';    unit = 'uJy'
#   name = 'ACS_F814W_FLUXERR'; unit = 'uJy'
#   name = 'ACS_F814W_MAG';    unit = 'mag'
#   name = 'ACS_F814W_MAGERR'; unit = 'mag'

ACS morphology
#   name = 'ACS_A_WORLD'; unit = 'deg'
#   name = 'ACS_B_WORLD'; unit = 'deg'
#   name = 'ACS_THETA_WORLD'; unit = 'deg'
#   name = 'ACS_FWHM_WORLD'; unit = 'deg'
#   name = 'ACS_MU_MAX'; unit = 'mag'
#   name = 'ACS_MU_CLASS'

#####################################################

Chandra COSMOS-Legacy Survey (Civano et al. 2016, Marchesi et al. 2016)

Matched identifier
#   name = 'ID_CHANDRA'

#####################################################

Corresponding Farmer source

Matched identifier
#   name = 'ID_FARMER'
```

```
#####################################################
Le Phare photo-z and physical parameters
#####################################################
# NOTE: MW correction derived from Schlafly&Finkbeiner+2011 values assuming Allen+1976 reddening

Photometric Redshift
Derived using a method similar to Ilbert et al. (2009, 2013)
#  name = 'lp_zBEST'

   z = zPDF  if galaxy  (median of the likelihood distribution)
   z = NaN   if star, Xray source based on Chandra (Civiano program), or masked area (FLAG_HSC|FLAG_SC|FLAG_UVISTA)

Star/Galaxy Separation
See paper for details
#  name = 'lp_type'

    type=0   if galaxy
    type=1   if star (mainly 3.6 micron, and half-light radius in HSC and HST)
    type=2   if Xray source
    type=-9  if failure in the fit (most of these objects have less than 1 band)



Best fit obtained with the galaxy templates
#  name = 'lp_zPDF'           photo-z (defined as the median of the likelihood) measured using the galaxy templates
#  name = 'lp_zPDF_l68'       lower limit, 68% confidence level
#  name = 'lp_zPDF_u68'       upper limit, 68% confidence level

#  name = 'lp_zMinChi2'       photo-z (defined as the minimum of the chi2) measured using the galaxy templates
#  name = 'lp_chi2_best'      reduced chi2 (-99 if less than 3 filters) for zMinChi2

#  name = 'lp_zp_2'           second photo-z solution if a second peak is detected with P>5% in the PDF
#  name = 'lp_chi2_2'         reduced chi2 for the second photo-z solution

#  name = 'lp_NbFilt'         Number of filters used in the fit

NOTE: Every source has a redshift, regardless of the type or if it is in a masked area or not

#########################################################

Best fit obtained with the AGN templates
#  name = 'lp_zq'             photoz for the AGN library.
#  name = 'lp_chiq'           reduced chi2
#  name = 'lp_modq'           best fit template

NOTE: This value is only informative: no correction for variability is applied.

#########################################################

Best fit obtained with the STAR templates

#  name = 'lp_mods'           model for the star library
#  name = 'lp_chis'           reduced chi2

#########################################################

Corresponding mask flag if masked by FLAG_UVISTA | FLAG_HSC | FLAG_SC

#  name = 'lp_mask'

#########################################################

Physical Properties
Derived from the BC03 best-fit templates at zPDF
(Chabrier IMF; cosmo:70,0.3,0.7; BC03 tau+delayed models described in Ilbert et al. 2015).
```

```
NOTE: A value is computed for all sources, even the one in masked area or classified as star

Best fit BC03 model at zPDF
#  name = 'lp_model'                    best-fit model index
#  name = 'lp_age'                      age of best-fit template in years
#  name = 'lp_dust'                     best-fit color excess E(B-V)
#  name = 'lp_Attenuation'              best-fit dust law index

Absolute rest-frame AB magnitudes
#  name = 'lp_MFUV'                  FUV galex
#  name = 'lp_MNUV'                  NUV galex
#  name = 'lp_MU'                    U  cfht new
#  name = 'lp_MG'                    g  Subaru HSC
#  name = 'lp_MR'                    r  Subaru HSC
#  name = 'lp_MI'                    i  Subaru HSC
#  name = 'lp_MZ'                    z  Subaru HSC
#  name = 'lp_MY'                    Y VISTA
#  name = 'lp_MJ'                    J VISTA
#  name = 'lp_MH'                    H VISTA
#  name = 'lp_MK'                    Ks VISTA

Galaxy Stellar Mass
#  name = 'lp_mass_med'           log Stellar mass from BC03 best-fit template. median of the PDF
#  name = 'lp_mass_med_min68'     lower limit, 68% confidence level
#  name = 'lp_mass_med_max68'     upper limit, 68% confidence level
#  name = 'lp_mass_best'          log Stellar mass from BC03 best-fit template. Taken at the minimum chi2

SFR and sSFR
#  name = 'lp_SFR_med'            log SFR from BC03 best-fit template. median of the PDF
#  name = 'lp_SFR_med_min68'      lower limit, 68% confidence level
#  name = 'lp_SFR_med_max68'      upper limit, 68% confidence level
#  name = 'lp_SFR_best'           log SFR from BC03 best-fit template. Taken at the minimum chi2

#  name = 'lp_sSFR_med'            log sSFR from BC03 best-fit template. median of the PDF
#  name = 'lp_sSFR_med_min68'      lower limit, 68% confidence level
#  name = 'lp_sSFR_med_max68'      upper limit, 68% confidence level
#  name = 'lp_sSFR_best'           log sSFR from BC03 best-fit template. Taken at the minimum chi2

NOTE: SFR and sSFR is computed without IR, large uncertainties with such methods

##################################################
EAZY photo-z and physical parameters
##################################################
NOTE: EAZY uses one value of Galactic extinction for all sources: E(B-V) = 0.017

Photometric redshift
Derived using the latest development version of eazy-py. See paper for details.
#  name = 'ez_z_phot'              maximum a-posteriori photometric redshift
#  name = 'ez_z_phot_chi2'         chi2 at z_phot, with z-prior
#  name = 'ez_z_phot_risk'         risk parameter from Tanaka+2018; R(ez_z_phot)
#  name = 'ez_z_min_risk'          redshift where R(z) is minimised
#  name = 'ez_min_risk'            R(ez_z_min_risk)
#  name = 'ez_z_raw_chi2'          redshift where chi2 is minimised, without priors
#  name = 'ez_raw_chi2'            chi2 at ez_z_raw_chi2

Redshift probability distribution percentiles
#  name = 'ez_z###'                     025, 160, 500, 840, 975 corresponds to 2.5%, 16%, 50%, 84%, 97.5%

Fitting parameters
#  name = 'ez_nusefilt'         number of filters used for photo-z (i.e., not masked as missing data)
#  name = 'ez_lc_min'           minimum effective wavelength of valid filters, Angstrom
#  name = 'ez_lc_max'           maximum effective wavelength of valid filters, Angstrom

Best-fit stellar templates
#  name = 'ez_star_min_chi2'    chi2 of best stellar template fit (BT-SETTL models); assumes 8% systematic uncertainty
```

```
#  name = 'ez_star_teff'        effective temperature of the stellar template; unit = 'K'

#########################################################

Physical Properties
Derived from the FSPS best-fit templates (Chabrier IMF; cosmo:69.4,0.287,0.713 - WMAP9).
Dust is applied by hand using the Kriek+Conroy attenuation curve (delta=0)
Total energy absorbed by this dust screen (energy_abs) is computed, and a corresponding far-IR component is added to
the SED using the templates from Magdis+2012.

Absolute rest-frame AB magnitudes
The templates are used to perform a weighted interpolation of the rest-frame filter by refitting the templates
at ez_z_phot but with the uncertainties weighted to favour observed-frame measurements closest to the desired rest-frame band.
#  name = 'ez_restU'                    rest-frame U-band flux (units of catalog fluxes, uJy)
#  name = 'ez_restU_err'                rest-frame U-band flux uncertainty (units of catalog fluxes, uJy)
#  name = 'ez_restB'                    rest-frame B-band flux (units of catalog fluxes, uJy)
#  name = 'ez_restB_err'                rest-frame B-band flux uncertainty (units of catalog fluxes, uJy)
#  name = 'ez_restV'                    rest-frame V-band flux (units of catalog fluxes, uJy)
#  name = 'ez_restV_err'                rest-frame V-band flux uncertainty (units of catalog fluxes, uJy)
#  name = 'ez_restJ'                    rest-frame J-band flux (units of catalog fluxes, uJy)
#  name = 'ez_restJ_err'                rest-frame J-band flux uncertainty (units of catalog fluxes, uJy)

Miscellaneous properties
#  name = 'ez_dL'                       luminosity distance at z_phot; unit = 'Mpc'
#  name = 'ez_mass'                     log(mass in Msun)
#  name = 'ez_sfr'                      log(sfr in Msun/yr)
#  name = 'ez_ssfr'                     log(ssfr in 1/yr)
#  name = 'ez_Lv'                       log(V-band luminosity in Lsun)
#  name = 'ez_LIR'                      total 8-1000um luminosity in Lsun)
#  name = 'ez_energy_abs'               implied absorbed energy associated with Av; unit = 'Lsun'
#  name = 'ez_Lu'                       luminosity in U-band; unit = 'Lsun'
#  name = 'ez_Lj'                       luminosity in J-band; unit = 'Lsun'
#  name = 'ez_L1400'                    luminosity tophat filter at 1400 A; unit = 'Lsun'
#  name = 'ez_L2800'                    luminosity tophat filter at 2800 A; unit = 'Lsun'
#  name = 'ez_LHa'                      Ha line luminosity (reddened), unit = 'Lsun'
#  name = 'ez_LOIII'                    OIII line luminosity (reddened), unit = 'Lsun'
#  name = 'ez_LHb'                      Hb line luminosity (reddened), unit = 'Lsun'
#  name = 'ez_LOII'                     OII line luminosity (reddened), unit = 'Lsun'
#  name = 'ez_MLv'                      mass-to-light ratio in V-band; unit = 'Msun/Lsun'
#  name = 'ez_Av'                       extinction in V-band; unit = 'Mag'
#  name = 'ez_lwAgeV'           light-weighted age in the V-band; unit = 'Gyr'

Property percentiles
Five percentiles (025, 160, 500, 840, 975 corresponds to 2.5%, 16%, 50%, 84%, 97.5%) are computed for:
ez_mass, ez_sfr, ez_ssfr, ez_Lv, ez_LIR, ez_energy_abs, ez_Lu, ez_Lj, ez_L1400, ez_L2800, ez_L2800, ez_Ha, ez_OIII,
ez_Hb, ez_OII. All are stated in the same scaling and units as their non-percentile columns.
#  name = 'ez_XXXX_p###'
```

4.4 The Farmer catalogue

The Farmer catalogue contains 430 columns and 964,506 rows. We provide matches with ACS, X-Ray, UV, IR, FIR and radio catalogues and also with previous COSMOS catalogues and in particular COSMOS2015. Sect. 4.5 provides the README file distributed with the catalogue describing each column. Additionally, in Sect. 6.2 we list of all the 430 columns together with their number, name, and description.

4.5 Description of The Farmer catalogue columns

```
The FARMER COSMOS2020 photometric catalog
```

```
We present here the catalog containing the photometry detected with SEP on a izYJHKs CHI-MEAN image
and extracted with The Tractor for about 1,000,000 sources in the COSMOS field within the areas of
UltraVISTA and outside the HSC bright star haloes. Suitable models are determined with izYJHKs imaging
for all detected sources, convolved with the PSF of a given band and optimised to measure flux
which is treated as a free parameter. Model parameters (radius, shape, etc.) are available upon request.
The full description of this catalog is in Weaver et al., 2022a (ApJS 258 11)

Updated 02/2022
contact: john.weaver.astro@gmail.com

########################################################
Identification
########################################################

Identifier
#   name = 'ID'

Right Ascension and Declination
#   name = 'ALPHA_J2000'; unit = 'deg'
#   name = 'DELTA_J2000'; unit = 'deg'

Coordinates above are based on model centroids, or SEP when models not available

Position, as determined by model centroid
#   name = 'X_MODEL'; unit = 'pixel'
#   name = 'Y_MODEL'; unit = 'pixel'
#   name = 'ERRX_MODEL'; unit = 'pixel'
#   name = 'ERRY_MODEL'; unit = 'pixel'

Position, as determined by SEP at detection, in J2000
#   name = 'ALPHA_DETECTION'; unit = 'deg'
#   name = 'DEC_DETECTION'; unit = 'deg'

Farmer model information
#   name = 'FARMER_ID'       Farmer internal source identifier ({brick}_{source})
#   name = 'GROUP_ID'        Farmer group identifier; unique within a brick
#   name = 'N_GROUP'         Farmer group occupation number
#   name = 'MODEL_FLAG'      (0: OK, 1: failed to converge, 2: drifted >0.6" from detection)
#   name = 'SOLUTION_MODEL'  The Tractor model type selected by The Farmer

Model shape information may be provided in a future release.

########################################################
Flags
########################################################

Flag for the bright stars and edges of the HSC images
#   name = 'FLAG_HSC'      (0:clean, 1:masked)

Flag for the bright stars and edges of the Suprime-Cam images
#   name = 'FLAG_SUPCAM'   (0:clean, 1:masked)

Flag for the UltraVISTA region
#   name = 'FLAG_UVISTA'   (0:inside, 1:outside)

Flag for the UltraVISTA ultra-deep regions
#   name = 'FLAG_UDEEP'    (0:ultra-deep, 1:deep)

Flag for the combination of FLAG_UVISTA, FLAG_HSC and FLAG_SUPCAM
#   name = 'FLAG_COMBINED' (0:clean and inside UVISTA)

########################################################
Galactic extinction at the object position
########################################################
```

```
E(B-V) values from Schlegel, Finkbeiner & Davis (1998) dust map
By default, a scaling of 0.86 is applied to the map values
to reflect the recalibration by Schlafly & Finkbeiner (2011)

#   name = 'EBV_MW'; unit = 'mag'

#########################################################
Photometry
#########################################################

No data convention
flux, fluxerr, mag, magerr = NaN

Negative flux convention
mag, magerr = NaN

NOTE: The photometry are not corrected for Milky Way extinction.
NOTE: The photometry are not corrected for photometric offsets derived by LePhare or EAZY
NOTE: The photometry errors are not corrected for the correlated noise in the images.

#########################################################

List of bands
CFHT/MegaCam (CLAUDS): ustar, u
Subaru/HSC: g, r, i, z, y
VISTA/VIRCAM (UltraVISTA DR4): Y, J, H, Ks, NB118
Subaru/Suprime-Cam: IB427, IB464, IA484, IB505, IA527, IB574, IA624, IA679, IB709, IA738,
                    IA767, IB827, NB711, NB816
Sptizer/IRAC (Cosmic DAWN Survey): IRAC_CH1, IRAC_CH2, IRAC_CH3, IRAC_CH4

NOTE: SuprimeCam Broad bands are not measured with Farmer

Total model fluxes, flux errors, magnitudes and magnitude errors
#   name = '###_FLUX';    unit = 'uJy'
#   name = '###_FLUXERR'; unit = 'uJy'
#   name = '###_MAG';    unit = 'mag'
#   name = '###_MAGERR'; unit = 'mag'

NOTE: aperture corrections should not be applied


#   name = '###_CHISQ'  Reduced Chi2 goodness of fit statistic for source profile model
#   name = '###_DRIFT'  Distance travelled from ALPHA/DELTA_J2000 (i.e. model centroid)
#   name = '###_VALID'  Set to False where FLUX or FLUXERR not trustworthy

#   name = 'VALID_SOURCE'    Set to False when photometry failed
#   name = 'SOLUTION_MODEL'  The Tractor model type selected by The Farmer

#########################################################
Ancillary photometry

NOTE: All are matched within 0.6" radius
#########################################################

GALEX photometry (Zamojski et al. 2007) from the Capak et al. 2007 catalog

Matched identifier
#   name = 'ID_GALEX'

List of bands
  GALEX_NUV, GALEX_FUV

#   name = '###_FLUX';    unit = 'uJy'
#   name = '###_FLUXERR'; unit = 'uJy'
```

```
#   name = '###_MAG';    unit = 'mag'
#   name = '###_MAGERR'; unit = 'mag'

#####################################################

SPLASH photometry from the COSMOS2015 catalog (Laigle et al. 2016)

Matched identifier
#   name = 'ID_COSMOS2015'

List of bands
  SPLASH_CH1, SPLASH_CH2, SPLASH_CH3, SPLASH_CH4

#   name = '###_FLUX';    unit = 'uJy'
#   name = '###_FLUXERR'; unit = 'uJy'
#   name = '###_MAG';    unit = 'mag'
#   name = '###_MAGERR'; unit = 'mag'

#####################################################

HST/ACS catalog (Leauthaud et al. 2007)
selection: CLEAN == 1

Matched identifier
#   name = 'ID_ACS'

ACS photometry
#   name = 'ACS_F814W_FLUX';    unit = 'uJy'
#   name = 'ACS_F814W_FLUXERR'; unit = 'uJy'
#   name = 'ACS_F814W_MAG';    unit = 'mag'
#   name = 'ACS_F814W_MAGERR'; unit = 'mag'

ACS morphology
#   name = 'ACS_A_WORLD'; unit = 'deg'
#   name = 'ACS_B_WORLD'; unit = 'deg'
#   name = 'ACS_THETA_WORLD'; unit = 'deg'
#   name = 'ACS_FWHM_WORLD'; unit = 'deg'
#   name = 'ACS_MU_MAX'; unit = 'mag'
#   name = 'ACS_MU_CLASS'

#####################################################

Chandra COSMOS-Legacy Survey (Civano et al. 2016, Marchesi et al. 2016)

Matched identifier
#   name = 'ID_CHANDRA'

#####################################################

Corresponding Classic 2020 source

Matched identifier
#   name = 'ID_CLASSIC'

#####################################################
Le Phare photo-z and physical parameters
#####################################################
# NOTE: MW correction derived from Schlafly&Finkbeiner+2011 values assuming Allen+1976 reddening

Photometric Redshift
Derived using a method similar to Ilbert et al. (2009, 2013)
#  name = 'lp_zBEST'

   z = zPDF  if galaxy  (median of the likelihood distribution)
   z = NaN   if star, Xray source based on Chandra (Civiano program), or masked area (FLAG_HSC|FLAG_SC|FLAG_UVISTA)
```

```
Star/Galaxy Separation
See paper for details
#  name = 'lp_type'

    type=0   if galaxy
    type=1   if star (mainly 3.6 micron, and half-light radius in HSC and HST)
    type=2   if Xray source
    type=-9  if failure in the fit (most of these objects have less than 1 band)



Best fit obtained with the galaxy templates
#  name = 'lp_zPDF'           photo-z (defined as the median of the likelihood) measured using the galaxy templates
#  name = 'lp_zPDF_l68'       lower limit, 68% confidence level
#  name = 'lp_zPDF_u68'       upper limit, 68% confidence level

#  name = 'lp_zMinChi2'       photo-z (defined as the minimum of the chi2) measured using the galaxy templates
#  name = 'lp_chi2_best'      reduced chi2 (-99 if less than 3 filters) for zMinChi2

#  name = 'lp_zp_2'           second photo-z solution if a second peak is detected with P>5% in the PDF
#  name = 'lp_chi2_2'         reduced chi2 for the second photo-z solution

#  name = 'lp_NbFilt'         Number of filters used in the fit

NOTE: Every source has a redshift, regardless of the type or if it is in a masked area or not

#########################################################

Best fit obtained with the AGN templates
#  name = 'lp_zq'             photoz for the AGN library.
#  name = 'lp_chiq'           reduced chi2
#  name = 'lp_modq'           best fit template

NOTE: This value is only informative: no correction for variability is applied.

#########################################################

Best fit obtained with the STAR templates

#  name = 'lp_mods'           model for the star library
#  name = 'lp_chis'           reduced chi2

#########################################################

Corresponding mask flag if masked by FLAG_UVISTA | FLAG_HSC | FLAG_SC

#  name = 'lp_mask'

#########################################################

Physical Properties
Derived from the BC03 best-fit templates at zPDF
(Chabrier IMF; cosmo:70,0.3,0.7; BC03 tau+delayed models described in Ilbert et al. 2015).
NOTE: A value is computed for all sources, even the one in masked area or classified as star

Best fit BC03 model at zPDF
#  name = 'lp_model'                  best-fit model index
#  name = 'lp_age'                    age of best-fit template in years
#  name = 'lp_dust'                   best-fit color excess E(B-V)
#  name = 'lp_Attenuation'            best-fit dust law index

Absolute rest-frame AB magnitudes
#  name = 'lp_MFUV'                FUV galex
#  name = 'lp_MNUV'                NUV galex
```

```
#  name = 'lp_MU'                  U  cfht new
#  name = 'lp_MG'                  g  Subaru HSC
#  name = 'lp_MR'                  r  Subaru HSC
#  name = 'lp_MI'                  i  Subaru HSC
#  name = 'lp_MZ'                  z  Subaru HSC
#  name = 'lp_MY'                  Y VISTA
#  name = 'lp_MJ'                  J VISTA
#  name = 'lp_MH'                  H VISTA
#  name = 'lp_MK'                  Ks VISTA

Galaxy Stellar Mass
#  name = 'lp_mass_med'           log Stellar mass from BC03 best-fit template. median of the PDF
#  name = 'lp_mass_med_min68'     lower limit, 68% confidence level
#  name = 'lp_mass_med_max68'     upper limit, 68% confidence level
#  name = 'lp_mass_best'          log Stellar mass from BC03 best-fit template. Taken at the minimum chi2

SFR and sSFR
#  name = 'lp_SFR_med'            log SFR from BC03 best-fit template. median of the PDF
#  name = 'lp_SFR_med_min68'      lower limit, 68% confidence level
#  name = 'lp_SFR_med_max68'      upper limit, 68% confidence level
#  name = 'lp_SFR_best'           log SFR from BC03 best-fit template. Taken at the minimum chi2

#  name = 'lp_sSFR_med'            log sSFR from BC03 best-fit template. median of the PDF
#  name = 'lp_sSFR_med_min68'      lower limit, 68% confidence level
#  name = 'lp_sSFR_med_max68'      upper limit, 68% confidence level
#  name = 'lp_sSFR_best'           log sSFR from BC03 best-fit template. Taken at the minimum chi2

NOTE: SFR and sSFR is computed without IR, large uncertainties with such methods

####################################################
EAZY photo-z and physical parameters
####################################################
NOTE: EAZY uses one value of Galactic extinction for all sources: E(B-V) = 0.017

Photometric redshift
Derived using the latest development version of eazy-py. See paper for details.
#  name = 'ez_z_phot'              maximum a-posteriori photometric redshift
#  name = 'ez_z_phot_chi2'         chi2 at z_phot, with z-prior
#  name = 'ez_z_phot_risk'         risk parameter from Tanaka+2018; R(ez_z_phot)
#  name = 'ez_z_min_risk'          redshift where R(z) is minimised
#  name = 'ez_min_risk'         R(ez_z_min_risk)
#  name = 'ez_z_raw_chi2'              redshift where chi2 is minimised, without priors
#  name = 'ez_raw_chi2'         chi2 at ez_z_raw_chi2

Redshift probability distribution percentiles
#  name = 'ez_z###'                    025, 160, 500, 840, 975 corresponds to 2.5%, 16%, 50%, 84%, 97.5%

Fitting parameters
#  name = 'ez_nusefilt'         number of filters used for photo-z (i.e., not masked as missing data)
#  name = 'ez_lc_min'           minimum effective wavelength of valid filters, Angstrom
#  name = 'ez_lc_max'           maximum effective wavelength of valid filters, Angstrom

Best-fit stellar templates
#  name = 'ez_star_min_chi2'    chi2 of best stellar template fit (BT-SETTL models); assumes 8% systematic uncertainty
#  name = 'ez_star_teff'        effective temperature of the stellar template; unit = 'K'

####################################################

Physical Properties
Derived from the FSPS best-fit templates (Chabrier IMF; cosmo:69.4,0.287,0.713 - WMAP9).
Dust is applied by hand using the Kriek+Conroy attenuation curve (delta=0)
Total energy absorbed by this dust screen (energy_abs) is computed, and a corresponding far-IR component is added to
the SED using the templates from Magdis+2012.

Absolute rest-frame AB magnitudes
```

```
The templates are used to perform a weighted interpolation of the rest-frame filter by refitting the templates
at ez_z_phot but with the uncertainties weighted to favour observed-frame measurements closest to the desired rest-frame band.
#  name = 'ez_restU'                    rest-frame U-band flux (units of catalog fluxes, uJy)
#  name = 'ez_restU_err'                rest-frame U-band flux uncertainty (units of catalog fluxes, uJy)
#  name = 'ez_restB'                    rest-frame B-band flux (units of catalog fluxes, uJy)
#  name = 'ez_restB_err'                rest-frame B-band flux uncertainty (units of catalog fluxes, uJy)
#  name = 'ez_restV'                    rest-frame V-band flux (units of catalog fluxes, uJy)
#  name = 'ez_restV_err'                rest-frame V-band flux uncertainty (units of catalog fluxes, uJy)
#  name = 'ez_restJ'                    rest-frame J-band flux (units of catalog fluxes, uJy)
#  name = 'ez_restJ_err'                rest-frame J-band flux uncertainty (units of catalog fluxes, uJy)

Miscellaneous properties
#  name = 'ez_dL'                       luminosity distance at z_phot; unit = 'Mpc'
#  name = 'ez_mass'                     log(mass in Msun)
#  name = 'ez_sfr'                      log(sfr in Msun/yr)
#  name = 'ez_ssfr'                     log(ssfr in 1/yr)
#  name = 'ez_Lv'                       log(V-band luminosity in Lsun)
#  name = 'ez_LIR'                      total 8-1000um luminosity in Lsun)
#  name = 'ez_energy_abs'               implied absorbed energy associated with Av; unit = 'Lsun'
#  name = 'ez_Lu'                       luminosity in U-band; unit = 'Lsun'
#  name = 'ez_Lj'                       luminosity in J-band; unit = 'Lsun'
#  name = 'ez_L1400'                    luminosity tophat filter at 1400 A; unit = 'Lsun'
#  name = 'ez_L2800'                    luminosity tophat filter at 2800 A; unit = 'Lsun'
#  name = 'ez_LHa'                      Ha line luminosity (reddened), unit = 'Lsun'
#  name = 'ez_LOIII'                    OIII line luminosity (reddened), unit = 'Lsun'
#  name = 'ez_LHb'                      Hb line luminosity (reddened), unit = 'Lsun'
#  name = 'ez_LOII'                     OII line luminosity (reddened), unit = 'Lsun'
#  name = 'ez_MLv'                      mass-to-light ratio in V-band; unit = 'Msun/Lsun'
#  name = 'ez_Av'                       extinction in V-band; unit = 'Mag'
#  name = 'ez_lwAgeV'                   light-weighted age in the V-band; unit = 'Gyr'

Property percentiles
Five percentiles (025, 160, 500, 840, 975 corresponds to 2.5%, 16%, 50%, 84%, 97.5%) are computed for the following properties:
ez_mass, ez_sfr, ez_ssfr, ez_Lv, ez_LIR, ez_energy_abs, ez_Lu, ez_Lj, ez_L1400, ez_L2800, ez_L2800, ez_Ha, ez_OIII,
ez_Hb, ez_OII. All are stated in the same scaling and units as their non-percentile columns.
#  name = 'ez_XXXX_p###'
```

4.6 Masks

In the COSMOS2020 catalogues, binary flags are used to identify different regions. Four areas are indicated: the region covered by the UltraVISTA survey (`FLAG_UVISTA`), the region covered by 'ultra-deep' stripes within the UltraVISTA survey (`FLAG_UDEEP`), the area covered by bright stars in the HSC survey (`FLAG_HSC`) and the area covered by bright stars in the legacy Suprime-cam data (`FLAG_SUPCAM`). Throughout, the same convention is used: for objects with `flag == 1` the object is within the masked region and should not be used. Objects with `flag == 0` are outside the masked region. These different masks are summarized in Table 5 and graphically in Figure 1. Also listed are the `ds9`[9] region files which are being made available with this release.

4.7 Redshift probability distributions

For each source, in both catalogues, we provide the redshift probability distributions or $p(z)$. These are stored as fits files.

The $p(z)$ results from `LePhare` are recorded as the likelihood at a given redshift spanning a baseline from $z = 0$ to 10 sampling in 1001 points of equal-z.

[9] `sites.google.com/cfa.harvard.edu/saoimageds9/home`

Table 5: A summary of the flags provided in the catalogue together with their associated region files.

Mask name	Area (deg^2)	Region file
FLAG_HSC	2.75	MASK_HSC-stars_griz.reg
FLAG_UVISTA	1.792	MASK_UVISTA.reg
FLAG_UDEEP	1.054	MASK_UDEEP.reg
FLAG_SUPCAM	1.918	MASK_SUPCAM.reg
FLAG_COMBINED	1.27	(all of the above except UDEEP)

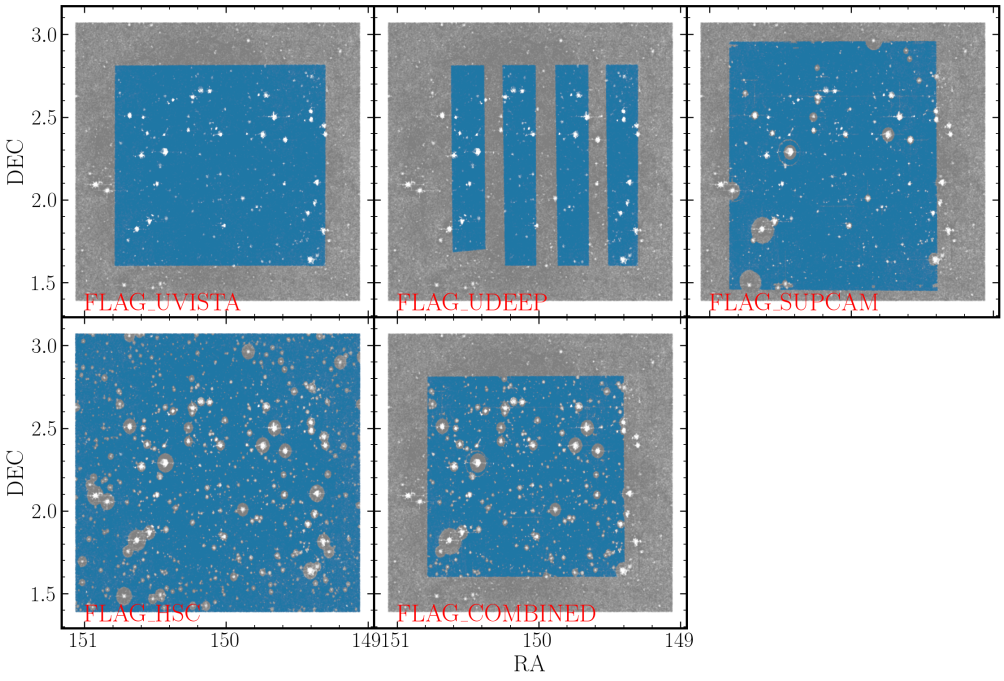

Figure 1: An illustration of the areas covered by each of the five different mask types present in the catalogue. Blue regions show the zones covered by the masks.

Slightly differently, the $p(z)$ results from `EAZY` are stored instead as 50 samplings of the cumulative redshift probability distribution or $cdf(z)$, equally spaced according to multiples of the standard deviation of a Gaussian distribution. As such, the $p(z)$ can be easily reconstructed from the relatively more compact $cdf(z)$ data without a significant loss of precision. Alternatively, users may find it advantageous to simply assess the probability of a source being in a certain redshift range by taking the difference in the $cdf(z)$ at two z points, equivalent to integrating the $p(z)$ but with much less computational effort. A script is provided to help users access and use this format.

4.8 Other products

Before photometric redshift measurements are made from photometric data, a series of corrections are applied to each object. These include correction of Milky Way extinction based on the value of $E(B-V)$ derived from dust maps and the application of a series of aperture offsets to bring individual colours to total photometry. At the release website, CLASSIC catalogue, we provide a `Python` program to compute this offset.

5 Acknowledgements

A full list of acknowledgements for the data sources used in this catalogue, together with their associated bibliographic references, can be found in Weaver et al. (2022).

6 Appendices

6.1 Complete list of Classic catalogue columns

The following is a list of number, name, description and unit for all the columns in CLASSIC.

No.	Column name	Column description	Column unit
1	ID	ID (specifically ID_CLASSIC, as this is the Classic catalogue)	
2	ALPHA_J2000	Right ascension (J2000)	deg
3	DELTA_J2000	Declination (J2000)	deg
4	X_IMAGE	Object position along X, with the scale being 0.15"/px	pix
5	Y_IMAGE	Object position along Y, with the scale being 0.15"/px	pix
6	ERRX2_IMAGE	Variance of position along X	pix**2
7	ERRY2_IMAGE	Variance of position along Y	pix**2
8	ERRXY_IMAGE	Covariance of position X / Y	pix**2
9	FLUX_RADIUS	Radius enclosing 50% of total flux in PSF-homogenized Ks-band image	pix
10	KRON_RADIUS	Reduced pseudo-radius derived from the izYJHKs detection image	
11	FLAG_HSC	Flag indicating quality of HSC imaging (0:clean, 1:masked)	
12	FLAG_SUPCAM	Flag indicating quality of Suprime-Cam imaging (0:clean, 1:masked)	
13	FLAG_UVISTA	Flag for the UltraVISTA region (0:inside, 1:outside)	
14	FLAG_UDEEP	Flag for the UltraVISTA ultra-deep regions (0:ultra-deep, 1:deep)	
15	FLAG_COMBINED	Comb. FLAG_UVISTA, FLAG_HSC, FLAG_SUPCAM (0:clean and inside UVISTA)	
16	EBV_MW	Galactic reddening E(B-V) (Schlegel+1998, Schlafly&Finkbeiner 2011)	
17	CFHT_u_FLUX_APER2	CFHT_u 2 arcsec diameter aperture flux density	uJy
18	CFHT_u_FLUXERR_APER2	CFHT_u 2 arcsec diameter aperture flux density error	uJy
19	CFHT_u_FLUX_APER3	CFHT_u 3 arcsec diameter aperture flux density	uJy
20	CFHT_u_FLUXERR_APER3	CFHT_u 3 arcsec diameter aperture flux density error	uJy

21	CFHT_u_FLUX_AUTO	CFHT_u AUTO flux density	uJy
22	CFHT_u_FLUXERR_AUTO	CFHT_u AUTO flux density error	uJy
23	CFHT_u_MAG_APER2	CFHT_u 2 arcsec diameter aperture AB magnitude	mag
24	CFHT_u_MAGERR_APER2	CFHT_u 2 arcsec diameter aperture AB magnitude error	mag
25	CFHT_u_MAG_APER3	CFHT_u 3 arcsec diameter aperture AB magnitude	mag
26	CFHT_u_MAGERR_APER3	CFHT_u 3 arcsec diameter aperture AB magnitude error	mag
27	CFHT_u_MAG_AUTO	CFHT_u AUTO AB magnitude	mag
28	CFHT_u_MAGERR_AUTO	CFHT_u AUTO AB magnitude error	mag
29	CFHT_u_MAG_ISO	CFHT_u ISO AB magnitude	mag
30	CFHT_u_MAGERR_ISO	CFHT_u ISO AB magnitude error	mag
31	CFHT_u_FLAGS	CFHT_u Source Extractor internal flags	
32	CFHT_u_IMAFLAGS_ISO	CFHT_u flags: 4 means saturated pixel(s) in the isophotal area	
33	CFHT_ustar_FLUX_APER2	CFHT_ustar 2 arcsec diameter aperture flux density	uJy
34	CFHT_ustar_FLUXERR_APER2	CFHT_ustar 2 arcsec diameter aperture flux density error	uJy
35	CFHT_ustar_FLUX_APER3	CFHT_ustar 3 arcsec diameter aperture flux density	uJy
36	CFHT_ustar_FLUXERR_APER3	CFHT_ustar 3 arcsec diameter aperture flux density error	uJy
37	CFHT_ustar_FLUX_AUTO	CFHT_ustar AUTO flux density	uJy
38	CFHT_ustar_FLUXERR_AUTO	CFHT_ustar AUTO flux density error	uJy
39	CFHT_ustar_MAG_APER2	CFHT_ustar 2 arcsec diameter aperture AB magnitude	mag
40	CFHT_ustar_MAGERR_APER2	CFHT_ustar 2 arcsec diameter aperture AB magnitude error	mag
41	CFHT_ustar_MAG_APER3	CFHT_ustar 3 arcsec diameter aperture AB magnitude	mag
42	CFHT_ustar_MAGERR_APER3	CFHT_ustar 3 arcsec diameter aperture AB magnitude error	mag
43	CFHT_ustar_MAG_AUTO	CFHT_ustar AUTO AB magnitude	mag
44	CFHT_ustar_MAGERR_AUTO	CFHT_ustar AUTO AB magnitude error	mag
45	CFHT_ustar_MAG_ISO	CFHT_ustar ISO AB magnitude	mag
46	CFHT_ustar_MAGERR_ISO	CFHT_ustar ISO AB magnitude error	mag
47	CFHT_ustar_FLAGS	CFHT_ustar Source Extractor internal flags	
48	CFHT_ustar_IMAFLAGS_ISO	CFHT_ustar flags: 4 means saturated pixel(s) in the isophotal area	
49	HSC_g_FLUX_APER2	HSC_g 2 arcsec diameter aperture flux density	uJy
50	HSC_g_FLUXERR_APER2	HSC_g 2 arcsec diameter aperture flux density error	uJy
51	HSC_g_FLUX_APER3	HSC_g 3 arcsec diameter aperture flux density	uJy
52	HSC_g_FLUXERR_APER3	HSC_g 3 arcsec diameter aperture flux density error	uJy
53	HSC_g_FLUX_AUTO	HSC_g AUTO flux density	uJy
54	HSC_g_FLUXERR_AUTO	HSC_g AUTO flux density error	uJy
55	HSC_g_MAG_APER2	HSC_g 2 arcsec diameter aperture AB magnitude	mag
56	HSC_g_MAGERR_APER2	HSC_g 2 arcsec diameter aperture AB magnitude error	mag
57	HSC_g_MAG_APER3	HSC_g 3 arcsec diameter aperture AB magnitude	mag
58	HSC_g_MAGERR_APER3	HSC_g 3 arcsec diameter aperture AB magnitude error	mag
59	HSC_g_MAG_AUTO	HSC_g AUTO AB magnitude	mag
60	HSC_g_MAGERR_AUTO	HSC_g AUTO AB magnitude error	mag
61	HSC_g_MAG_ISO	HSC_g ISO AB magnitude	mag
62	HSC_g_MAGERR_ISO	HSC_g ISO AB magnitude error	mag
63	HSC_g_FLAGS	HSC_g Source Extractor internal flags	
64	HSC_g_IMAFLAGS_ISO	HSC_g flags: 4 means saturated pixel(s) in the isophotal area	
65	HSC_r_FLUX_APER2	HSC_r 2 arcsec diameter aperture flux density	uJy
66	HSC_r_FLUXERR_APER2	HSC_r 2 arcsec diameter aperture flux density error	uJy
67	HSC_r_FLUX_APER3	HSC_r 3 arcsec diameter aperture flux density	uJy
68	HSC_r_FLUXERR_APER3	HSC_r 3 arcsec diameter aperture flux density error	uJy
69	HSC_r_FLUX_AUTO	HSC_r AUTO flux density	uJy
70	HSC_r_FLUXERR_AUTO	HSC_r AUTO flux density error	uJy
71	HSC_r_MAG_APER2	HSC_r 2 arcsec diameter aperture AB magnitude	mag
72	HSC_r_MAGERR_APER2	HSC_r 2 arcsec diameter aperture AB magnitude error	mag
73	HSC_r_MAG_APER3	HSC_r 3 arcsec diameter aperture AB magnitude	mag
74	HSC_r_MAGERR_APER3	HSC_r 3 arcsec diameter aperture AB magnitude error	mag
75	HSC_r_MAG_AUTO	HSC_r AUTO AB magnitude	mag
76	HSC_r_MAGERR_AUTO	HSC_r AUTO AB magnitude error	mag
77	HSC_r_MAG_ISO	HSC_r ISO AB magnitude	mag
78	HSC_r_MAGERR_ISO	HSC_r ISO AB magnitude error	mag
79	HSC_r_FLAGS	HSC_r Source Extractor internal flags	
80	HSC_r_IMAFLAGS_ISO	HSC_r flags: 4 means saturated pixel(s) in the isophotal area	
81	HSC_i_FLUX_APER2	HSC_i 2 arcsec diameter aperture flux density	uJy
82	HSC_i_FLUXERR_APER2	HSC_i 2 arcsec diameter aperture flux density error	uJy
83	HSC_i_FLUX_APER3	HSC_i 3 arcsec diameter aperture flux density	uJy
84	HSC_i_FLUXERR_APER3	HSC_i 3 arcsec diameter aperture flux density error	uJy
85	HSC_i_FLUX_AUTO	HSC_i AUTO flux density	uJy

86	HSC_i_FLUXERR_AUTO	HSC_i AUTO flux density error	uJy
87	HSC_i_MAG_APER2	HSC_i 2 arcsec diameter aperture AB magnitude	mag
88	HSC_i_MAGERR_APER2	HSC_i 2 arcsec diameter aperture AB magnitude error	mag
89	HSC_i_MAG_APER3	HSC_i 3 arcsec diameter aperture AB magnitude	mag
90	HSC_i_MAGERR_APER3	HSC_i 3 arcsec diameter aperture AB magnitude error	mag
91	HSC_i_MAG_AUTO	HSC_i AUTO AB magnitude	mag
92	HSC_i_MAGERR_AUTO	HSC_i AUTO AB magnitude error	mag
93	HSC_i_MAG_ISO	HSC_i ISO AB magnitude	mag
94	HSC_i_MAGERR_ISO	HSC_i ISO AB magnitude error	mag
95	HSC_i_FLAGS	HSC_i Source Extractor internal flags	
96	HSC_i_IMAFLAGS_ISO	HSC_i flags: 4 means saturated pixel(s) in the isophotal area	
97	HSC_z_FLUX_APER2	HSC_z 2 arcsec diameter aperture flux density	uJy
98	HSC_z_FLUXERR_APER2	HSC_z 2 arcsec diameter aperture flux density error	uJy
99	HSC_z_FLUX_APER3	HSC_z 3 arcsec diameter aperture flux density	uJy
100	HSC_z_FLUXERR_APER3	HSC_z 3 arcsec diameter aperture flux density error	uJy
101	HSC_z_FLUX_AUTO	HSC_z AUTO flux density	uJy
102	HSC_z_FLUXERR_AUTO	HSC_z AUTO flux density error	uJy
103	HSC_z_MAG_APER2	HSC_z 2 arcsec diameter aperture AB magnitude	mag
104	HSC_z_MAGERR_APER2	HSC_z 2 arcsec diameter aperture AB magnitude error	mag
105	HSC_z_MAG_APER3	HSC_z 3 arcsec diameter aperture AB magnitude	mag
106	HSC_z_MAGERR_APER3	HSC_z 3 arcsec diameter aperture AB magnitude error	mag
107	HSC_z_MAG_AUTO	HSC_z AUTO AB magnitude	mag
108	HSC_z_MAGERR_AUTO	HSC_z AUTO AB magnitude error	mag
109	HSC_z_MAG_ISO	HSC_z ISO AB magnitude	mag
110	HSC_z_MAGERR_ISO	HSC_z ISO AB magnitude error	mag
111	HSC_z_FLAGS	HSC_z Source Extractor internal flags	
112	HSC_z_IMAFLAGS_ISO	HSC_z flags: 4 means saturated pixel(s) in the isophotal area	
113	HSC_y_FLUX_APER2	HSC_y 2 arcsec diameter aperture flux density	uJy
114	HSC_y_FLUXERR_APER2	HSC_y 2 arcsec diameter aperture flux density error	uJy
115	HSC_y_FLUX_APER3	HSC_y 3 arcsec diameter aperture flux density	uJy
116	HSC_y_FLUXERR_APER3	HSC_y 3 arcsec diameter aperture flux density error	uJy
117	HSC_y_FLUX_AUTO	HSC_y AUTO flux density	uJy
118	HSC_y_FLUXERR_AUTO	HSC_y AUTO flux density error	uJy
119	HSC_y_MAG_APER2	HSC_y 2 arcsec diameter aperture AB magnitude	mag
120	HSC_y_MAGERR_APER2	HSC_y 2 arcsec diameter aperture AB magnitude error	mag
121	HSC_y_MAG_APER3	HSC_y 3 arcsec diameter aperture AB magnitude	mag
122	HSC_y_MAGERR_APER3	HSC_y 3 arcsec diameter aperture AB magnitude error	mag
123	HSC_y_MAG_AUTO	HSC_y AUTO AB magnitude	mag
124	HSC_y_MAGERR_AUTO	HSC_y AUTO AB magnitude error	mag
125	HSC_y_MAG_ISO	HSC_y ISO AB magnitude	mag
126	HSC_y_MAGERR_ISO	HSC_y ISO AB magnitude error	mag
127	HSC_y_FLAGS	HSC_y Source Extractor internal flags	
128	HSC_y_IMAFLAGS_ISO	HSC_y flags: 4 means saturated pixel(s) in the isophotal area	
129	UVISTA_Y_FLUX_APER2	UVISTA_Y 2 arcsec diameter aperture flux density	uJy
130	UVISTA_Y_FLUXERR_APER2	UVISTA_Y 2 arcsec diameter aperture flux density error	uJy
131	UVISTA_Y_FLUX_APER3	UVISTA_Y 3 arcsec diameter aperture flux density	uJy
132	UVISTA_Y_FLUXERR_APER3	UVISTA_Y 3 arcsec diameter aperture flux density error	uJy
133	UVISTA_Y_FLUX_AUTO	UVISTA_Y AUTO flux density	uJy
134	UVISTA_Y_FLUXERR_AUTO	UVISTA_Y AUTO flux density error	uJy
135	UVISTA_Y_MAG_APER2	UVISTA_Y 2 arcsec diameter aperture AB magnitude	mag
136	UVISTA_Y_MAGERR_APER2	UVISTA_Y 2 arcsec diameter aperture AB magnitude error	mag
137	UVISTA_Y_MAG_APER3	UVISTA_Y 3 arcsec diameter aperture AB magnitude	mag
138	UVISTA_Y_MAGERR_APER3	UVISTA_Y 3 arcsec diameter aperture AB magnitude error	mag
139	UVISTA_Y_MAG_AUTO	UVISTA_Y AUTO AB magnitude	mag
140	UVISTA_Y_MAGERR_AUTO	UVISTA_Y AUTO AB magnitude error	mag
141	UVISTA_Y_MAG_ISO	UVISTA_Y ISO AB magnitude	mag
142	UVISTA_Y_MAGERR_ISO	UVISTA_Y ISO AB magnitude error	mag
143	UVISTA_Y_FLAGS	UVISTA_Y Source Extractor internal flags	
144	UVISTA_Y_IMAFLAGS_ISO	UVISTA_Y flags: 4 means saturated pixel(s) in the isophotal area	
145	UVISTA_J_FLUX_APER2	UVISTA_J 2 arcsec diameter aperture flux density	uJy
146	UVISTA_J_FLUXERR_APER2	UVISTA_J 2 arcsec diameter aperture flux density error	uJy
147	UVISTA_J_FLUX_APER3	UVISTA_J 3 arcsec diameter aperture flux density	uJy
148	UVISTA_J_FLUXERR_APER3	UVISTA_J 3 arcsec diameter aperture flux density error	uJy
149	UVISTA_J_FLUX_AUTO	UVISTA_J AUTO flux density	uJy
150	UVISTA_J_FLUXERR_AUTO	UVISTA_J AUTO flux density error	uJy

151	UVISTA_J_MAG_APER2	UVISTA_J 2 arcsec diameter aperture AB magnitude	mag
152	UVISTA_J_MAGERR_APER2	UVISTA_J 2 arcsec diameter aperture AB magnitude error	mag
153	UVISTA_J_MAG_APER3	UVISTA_J 3 arcsec diameter aperture AB magnitude	mag
154	UVISTA_J_MAGERR_APER3	UVISTA_J 3 arcsec diameter aperture AB magnitude error	mag
155	UVISTA_J_MAG_AUTO	UVISTA_J AUTO AB magnitude	mag
156	UVISTA_J_MAGERR_AUTO	UVISTA_J AUTO AB magnitude error	mag
157	UVISTA_J_MAG_ISO	UVISTA_J ISO AB magnitude	mag
158	UVISTA_J_MAGERR_ISO	UVISTA_J ISO AB magnitude error	mag
159	UVISTA_J_FLAGS	UVISTA_J Source Extractor internal flags	
160	UVISTA_J_IMAFLAGS_ISO	UVISTA_J flags: 4 means saturated pixel(s) in the isophotal area	
161	UVISTA_H_FLUX_APER2	UVISTA_H 2 arcsec diameter aperture flux density	uJy
162	UVISTA_H_FLUXERR_APER2	UVISTA_H 2 arcsec diameter aperture flux density error	uJy
163	UVISTA_H_FLUX_APER3	UVISTA_H 3 arcsec diameter aperture flux density	uJy
164	UVISTA_H_FLUXERR_APER3	UVISTA_H 3 arcsec diameter aperture flux density error	uJy
165	UVISTA_H_FLUX_AUTO	UVISTA_H AUTO flux density	uJy
166	UVISTA_H_FLUXERR_AUTO	UVISTA_H AUTO flux density error	uJy
167	UVISTA_H_MAG_APER2	UVISTA_H 2 arcsec diameter aperture AB magnitude	mag
168	UVISTA_H_MAGERR_APER2	UVISTA_H 2 arcsec diameter aperture AB magnitude error	mag
169	UVISTA_H_MAG_APER3	UVISTA_H 3 arcsec diameter aperture AB magnitude	mag
170	UVISTA_H_MAGERR_APER3	UVISTA_H 3 arcsec diameter aperture AB magnitude error	mag
171	UVISTA_H_MAG_AUTO	UVISTA_H AUTO AB magnitude	mag
172	UVISTA_H_MAGERR_AUTO	UVISTA_H AUTO AB magnitude error	mag
173	UVISTA_H_MAG_ISO	UVISTA_H ISO AB magnitude	mag
174	UVISTA_H_MAGERR_ISO	UVISTA_H ISO AB magnitude error	mag
175	UVISTA_H_FLAGS	UVISTA_H Source Extractor internal flags	
176	UVISTA_H_IMAFLAGS_ISO	UVISTA_H flags: 4 means saturated pixel(s) in the isophotal area	
177	UVISTA_Ks_FLUX_APER2	UVISTA_Ks 2 arcsec diameter aperture flux density	uJy
178	UVISTA_Ks_FLUXERR_APER2	UVISTA_Ks 2 arcsec diameter aperture flux density error	uJy
179	UVISTA_Ks_FLUX_APER3	UVISTA_Ks 3 arcsec diameter aperture flux density	uJy
180	UVISTA_Ks_FLUXERR_APER3	UVISTA_Ks 3 arcsec diameter aperture flux density error	uJy
181	UVISTA_Ks_FLUX_AUTO	UVISTA_Ks AUTO flux density	uJy
182	UVISTA_Ks_FLUXERR_AUTO	UVISTA_Ks AUTO flux density error	uJy
183	UVISTA_Ks_MAG_APER2	UVISTA_Ks 2 arcsec diameter aperture AB magnitude	mag
184	UVISTA_Ks_MAGERR_APER2	UVISTA_Ks 2 arcsec diameter aperture AB magnitude error	mag
185	UVISTA_Ks_MAG_APER3	UVISTA_Ks 3 arcsec diameter aperture AB magnitude	mag
186	UVISTA_Ks_MAGERR_APER3	UVISTA_Ks 3 arcsec diameter aperture AB magnitude error	mag
187	UVISTA_Ks_MAG_AUTO	UVISTA_Ks AUTO AB magnitude	mag
188	UVISTA_Ks_MAGERR_AUTO	UVISTA_Ks AUTO AB magnitude error	mag
189	UVISTA_Ks_MAG_ISO	UVISTA_Ks ISO AB magnitude	mag
190	UVISTA_Ks_MAGERR_ISO	UVISTA_Ks ISO AB magnitude error	mag
191	UVISTA_Ks_FLAGS	UVISTA_Ks Source Extractor internal flags	
192	UVISTA_Ks_IMAFLAGS_ISO	UVISTA_Ks flags: 4 means saturated pixel(s) in the isophotal area	
193	SC_IB427_FLUX_APER2	SC_IB427 2 arcsec diameter aperture flux density	uJy
194	SC_IB427_FLUXERR_APER2	SC_IB427 2 arcsec diameter aperture flux density error	uJy
195	SC_IB427_FLUX_APER3	SC_IB427 3 arcsec diameter aperture flux density	uJy
196	SC_IB427_FLUXERR_APER3	SC_IB427 3 arcsec diameter aperture flux density error	uJy
197	SC_IB427_FLUX_AUTO	SC_IB427 AUTO flux density	uJy
198	SC_IB427_FLUXERR_AUTO	SC_IB427 AUTO flux density error	uJy
199	SC_IB427_MAG_APER2	SC_IB427 2 arcsec diameter aperture AB magnitude	mag
200	SC_IB427_MAGERR_APER2	SC_IB427 2 arcsec diameter aperture AB magnitude error	mag
201	SC_IB427_MAG_APER3	SC_IB427 3 arcsec diameter aperture AB magnitude	mag
202	SC_IB427_MAGERR_APER3	SC_IB427 3 arcsec diameter aperture AB magnitude error	mag
203	SC_IB427_MAG_AUTO	SC_IB427 AUTO AB magnitude	mag
204	SC_IB427_MAGERR_AUTO	SC_IB427 AUTO AB magnitude error	mag
205	SC_IB427_MAG_ISO	SC_IB427 ISO AB magnitude	mag
206	SC_IB427_MAGERR_ISO	SC_IB427 ISO AB magnitude error	mag
207	SC_IB427_FLAGS	SC_IB427 Source Extractor internal flags	
208	SC_IB427_IMAFLAGS_ISO	SC_IB427 flags: 4 means saturated pixel(s) in the isophotal area	
209	SC_IB464_FLUX_APER2	SC_IB464 2 arcsec diameter aperture flux density	uJy
210	SC_IB464_FLUXERR_APER2	SC_IB464 2 arcsec diameter aperture flux density error	uJy
211	SC_IB464_FLUX_APER3	SC_IB464 3 arcsec diameter aperture flux density	uJy
212	SC_IB464_FLUXERR_APER3	SC_IB464 3 arcsec diameter aperture flux density error	uJy
213	SC_IB464_FLUX_AUTO	SC_IB464 AUTO flux density	uJy
214	SC_IB464_FLUXERR_AUTO	SC_IB464 AUTO flux density error	uJy
215	SC_IB464_MAG_APER2	SC_IB464 2 arcsec diameter aperture AB magnitude	mag

216	SC_IB464_MAGERR_APER2	SC_IB464 2 arcsec diameter aperture AB magnitude error	mag
217	SC_IB464_MAG_APER3	SC_IB464 3 arcsec diameter aperture AB magnitude	mag
218	SC_IB464_MAGERR_APER3	SC_IB464 3 arcsec diameter aperture AB magnitude error	mag
219	SC_IB464_MAG_AUTO	SC_IB464 AUTO AB magnitude	mag
220	SC_IB464_MAGERR_AUTO	SC_IB464 AUTO AB magnitude error	mag
221	SC_IB464_MAG_ISO	SC_IB464 ISO AB magnitude	mag
222	SC_IB464_MAGERR_ISO	SC_IB464 ISO AB magnitude error	mag
223	SC_IB464_FLAGS	SC_IB464 Source Extractor internal flags	
224	SC_IB464_IMAFLAGS_ISO	SC_IB464 flags: 4 means saturated pixel(s) in the isophotal area	
225	SC_IA484_FLUX_APER2	SC_IA484 2 arcsec diameter aperture flux density	uJy
226	SC_IA484_FLUXERR_APER2	SC_IA484 2 arcsec diameter aperture flux density error	uJy
227	SC_IA484_FLUX_APER3	SC_IA484 3 arcsec diameter aperture flux density	uJy
228	SC_IA484_FLUXERR_APER3	SC_IA484 3 arcsec diameter aperture flux density error	uJy
229	SC_IA484_FLUX_AUTO	SC_IA484 AUTO flux density	uJy
230	SC_IA484_FLUXERR_AUTO	SC_IA484 AUTO flux density error	uJy
231	SC_IA484_MAG_APER2	SC_IA484 2 arcsec diameter aperture AB magnitude	mag
232	SC_IA484_MAGERR_APER2	SC_IA484 2 arcsec diameter aperture AB magnitude error	mag
233	SC_IA484_MAG_APER3	SC_IA484 3 arcsec diameter aperture AB magnitude	mag
234	SC_IA484_MAGERR_APER3	SC_IA484 3 arcsec diameter aperture AB magnitude error	mag
235	SC_IA484_MAG_AUTO	SC_IA484 AUTO AB magnitude	mag
236	SC_IA484_MAGERR_AUTO	SC_IA484 AUTO AB magnitude error	mag
237	SC_IA484_MAG_ISO	SC_IA484 ISO AB magnitude	mag
238	SC_IA484_MAGERR_ISO	SC_IA484 ISO AB magnitude error	mag
239	SC_IA484_FLAGS	SC_IA484 Source Extractor internal flags	
240	SC_IA484_IMAFLAGS_ISO	SC_IA484 flags: 4 means saturated pixel(s) in the isophotal area	
241	SC_IB505_FLUX_APER2	SC_IB505 2 arcsec diameter aperture flux density	uJy
242	SC_IB505_FLUXERR_APER2	SC_IB505 2 arcsec diameter aperture flux density error	uJy
243	SC_IB505_FLUX_APER3	SC_IB505 3 arcsec diameter aperture flux density	uJy
244	SC_IB505_FLUXERR_APER3	SC_IB505 3 arcsec diameter aperture flux density error	uJy
245	SC_IB505_FLUX_AUTO	SC_IB505 AUTO flux density	uJy
246	SC_IB505_FLUXERR_AUTO	SC_IB505 AUTO flux density error	uJy
247	SC_IB505_MAG_APER2	SC_IB505 2 arcsec diameter aperture AB magnitude	mag
248	SC_IB505_MAGERR_APER2	SC_IB505 2 arcsec diameter aperture AB magnitude error	mag
249	SC_IB505_MAG_APER3	SC_IB505 3 arcsec diameter aperture AB magnitude	mag
250	SC_IB505_MAGERR_APER3	SC_IB505 3 arcsec diameter aperture AB magnitude error	mag
251	SC_IB505_MAG_AUTO	SC_IB505 AUTO AB magnitude	mag
252	SC_IB505_MAGERR_AUTO	SC_IB505 AUTO AB magnitude error	mag
253	SC_IB505_MAG_ISO	SC_IB505 ISO AB magnitude	mag
254	SC_IB505_MAGERR_ISO	SC_IB505 ISO AB magnitude error	mag
255	SC_IB505_FLAGS	SC_IB505 Source Extractor internal flags	
256	SC_IB505_IMAFLAGS_ISO	SC_IB505 flags: 4 means saturated pixel(s) in the isophotal area	
257	SC_IA527_FLUX_APER2	SC_IA527 2 arcsec diameter aperture flux density	uJy
258	SC_IA527_FLUXERR_APER2	SC_IA527 2 arcsec diameter aperture flux density error	uJy
259	SC_IA527_FLUX_APER3	SC_IA527 3 arcsec diameter aperture flux density	uJy
260	SC_IA527_FLUXERR_APER3	SC_IA527 3 arcsec diameter aperture flux density error	uJy
261	SC_IA527_FLUX_AUTO	SC_IA527 AUTO flux density	uJy
262	SC_IA527_FLUXERR_AUTO	SC_IA527 AUTO flux density error	uJy
263	SC_IA527_MAG_APER2	SC_IA527 2 arcsec diameter aperture AB magnitude	mag
264	SC_IA527_MAGERR_APER2	SC_IA527 2 arcsec diameter aperture AB magnitude error	mag
265	SC_IA527_MAG_APER3	SC_IA527 3 arcsec diameter aperture AB magnitude	mag
266	SC_IA527_MAGERR_APER3	SC_IA527 3 arcsec diameter aperture AB magnitude error	mag
267	SC_IA527_MAG_AUTO	SC_IA527 AUTO AB magnitude	mag
268	SC_IA527_MAGERR_AUTO	SC_IA527 AUTO AB magnitude error	mag
269	SC_IA527_MAG_ISO	SC_IA527 ISO AB magnitude	mag
270	SC_IA527_MAGERR_ISO	SC_IA527 ISO AB magnitude error	mag
271	SC_IA527_FLAGS	SC_IA527 Source Extractor internal flags	
272	SC_IA527_IMAFLAGS_ISO	SC_IA527 flags: 4 means saturated pixel(s) in the isophotal area	
273	SC_IB574_FLUX_APER2	SC_IB574 2 arcsec diameter aperture flux density	uJy
274	SC_IB574_FLUXERR_APER2	SC_IB574 2 arcsec diameter aperture flux density error	uJy
275	SC_IB574_FLUX_APER3	SC_IB574 3 arcsec diameter aperture flux density	uJy
276	SC_IB574_FLUXERR_APER3	SC_IB574 3 arcsec diameter aperture flux density error	uJy
277	SC_IB574_FLUX_AUTO	SC_IB574 AUTO flux density	uJy
278	SC_IB574_FLUXERR_AUTO	SC_IB574 AUTO flux density error	uJy
279	SC_IB574_MAG_APER2	SC_IB574 2 arcsec diameter aperture AB magnitude	mag
280	SC_IB574_MAGERR_APER2	SC_IB574 2 arcsec diameter aperture AB magnitude error	mag

281	SC_IB574_MAG_APER3	SC_IB574 3 arcsec diameter aperture AB magnitude	mag
282	SC_IB574_MAGERR_APER3	SC_IB574 3 arcsec diameter aperture AB magnitude error	mag
283	SC_IB574_MAG_AUTO	SC_IB574 AUTO AB magnitude	mag
284	SC_IB574_MAGERR_AUTO	SC_IB574 AUTO AB magnitude error	mag
285	SC_IB574_MAG_ISO	SC_IB574 ISO AB magnitude	mag
286	SC_IB574_MAGERR_ISO	SC_IB574 ISO AB magnitude error	mag
287	SC_IB574_FLAGS	SC_IB574 Source Extractor internal flags	
288	SC_IB574_IMAFLAGS_ISO	SC_IB574 flags: 4 means saturated pixel(s) in the isophotal area	
289	SC_IA624_FLUX_APER2	SC_IA624 2 arcsec diameter aperture flux density	uJy
290	SC_IA624_FLUXERR_APER2	SC_IA624 2 arcsec diameter aperture flux density error	uJy
291	SC_IA624_FLUX_APER3	SC_IA624 3 arcsec diameter aperture flux density	uJy
292	SC_IA624_FLUXERR_APER3	SC_IA624 3 arcsec diameter aperture flux density error	uJy
293	SC_IA624_FLUX_AUTO	SC_IA624 AUTO flux density	uJy
294	SC_IA624_FLUXERR_AUTO	SC_IA624 AUTO flux density error	uJy
295	SC_IA624_MAG_APER2	SC_IA624 2 arcsec diameter aperture AB magnitude	mag
296	SC_IA624_MAGERR_APER2	SC_IA624 2 arcsec diameter aperture AB magnitude error	mag
297	SC_IA624_MAG_APER3	SC_IA624 3 arcsec diameter aperture AB magnitude	mag
298	SC_IA624_MAGERR_APER3	SC_IA624 3 arcsec diameter aperture AB magnitude error	mag
299	SC_IA624_MAG_AUTO	SC_IA624 AUTO AB magnitude	mag
300	SC_IA624_MAGERR_AUTO	SC_IA624 AUTO AB magnitude error	mag
301	SC_IA624_MAG_ISO	SC_IA624 ISO AB magnitude	mag
302	SC_IA624_MAGERR_ISO	SC_IA624 ISO AB magnitude error	mag
303	SC_IA624_FLAGS	SC_IA624 Source Extractor internal flags	
304	SC_IA624_IMAFLAGS_ISO	SC_IA624 flags: 4 means saturated pixel(s) in the isophotal area	
305	SC_IA679_FLUX_APER2	SC_IA679 2 arcsec diameter aperture flux density	uJy
306	SC_IA679_FLUXERR_APER2	SC_IA679 2 arcsec diameter aperture flux density error	uJy
307	SC_IA679_FLUX_APER3	SC_IA679 3 arcsec diameter aperture flux density	uJy
308	SC_IA679_FLUXERR_APER3	SC_IA679 3 arcsec diameter aperture flux density error	uJy
309	SC_IA679_FLUX_AUTO	SC_IA679 AUTO flux density	uJy
310	SC_IA679_FLUXERR_AUTO	SC_IA679 AUTO flux density error	uJy
311	SC_IA679_MAG_APER2	SC_IA679 2 arcsec diameter aperture AB magnitude	mag
312	SC_IA679_MAGERR_APER2	SC_IA679 2 arcsec diameter aperture AB magnitude error	mag
313	SC_IA679_MAG_APER3	SC_IA679 3 arcsec diameter aperture AB magnitude	mag
314	SC_IA679_MAGERR_APER3	SC_IA679 3 arcsec diameter aperture AB magnitude error	mag
315	SC_IA679_MAG_AUTO	SC_IA679 AUTO AB magnitude	mag
316	SC_IA679_MAGERR_AUTO	SC_IA679 AUTO AB magnitude error	mag
317	SC_IA679_MAG_ISO	SC_IA679 ISO AB magnitude	mag
318	SC_IA679_MAGERR_ISO	SC_IA679 ISO AB magnitude error	mag
319	SC_IA679_FLAGS	SC_IA679 Source Extractor internal flags	
320	SC_IA679_IMAFLAGS_ISO	SC_IA679 flags: 4 means saturated pixel(s) in the isophotal area	
321	SC_IB709_FLUX_APER2	SC_IB709 2 arcsec diameter aperture flux density	uJy
322	SC_IB709_FLUXERR_APER2	SC_IB709 2 arcsec diameter aperture flux density error	uJy
323	SC_IB709_FLUX_APER3	SC_IB709 3 arcsec diameter aperture flux density	uJy
324	SC_IB709_FLUXERR_APER3	SC_IB709 3 arcsec diameter aperture flux density error	uJy
325	SC_IB709_FLUX_AUTO	SC_IB709 AUTO flux density	uJy
326	SC_IB709_FLUXERR_AUTO	SC_IB709 AUTO flux density error	uJy
327	SC_IB709_MAG_APER2	SC_IB709 2 arcsec diameter aperture AB magnitude	mag
328	SC_IB709_MAGERR_APER2	SC_IB709 2 arcsec diameter aperture AB magnitude error	mag
329	SC_IB709_MAG_APER3	SC_IB709 3 arcsec diameter aperture AB magnitude	mag
330	SC_IB709_MAGERR_APER3	SC_IB709 3 arcsec diameter aperture AB magnitude error	mag
331	SC_IB709_MAG_AUTO	SC_IB709 AUTO AB magnitude	mag
332	SC_IB709_MAGERR_AUTO	SC_IB709 AUTO AB magnitude error	mag
333	SC_IB709_MAG_ISO	SC_IB709 ISO AB magnitude	mag
334	SC_IB709_MAGERR_ISO	SC_IB709 ISO AB magnitude error	mag
335	SC_IB709_FLAGS	SC_IB709 Source Extractor internal flags	
336	SC_IB709_IMAFLAGS_ISO	SC_IB709 flags: 4 means saturated pixel(s) in the isophotal area	
337	SC_IA738_FLUX_APER2	SC_IA738 2 arcsec diameter aperture flux density	uJy
338	SC_IA738_FLUXERR_APER2	SC_IA738 2 arcsec diameter aperture flux density error	uJy
339	SC_IA738_FLUX_APER3	SC_IA738 3 arcsec diameter aperture flux density	uJy
340	SC_IA738_FLUXERR_APER3	SC_IA738 3 arcsec diameter aperture flux density error	uJy
341	SC_IA738_FLUX_AUTO	SC_IA738 AUTO flux density	uJy
342	SC_IA738_FLUXERR_AUTO	SC_IA738 AUTO flux density error	uJy
343	SC_IA738_MAG_APER2	SC_IA738 2 arcsec diameter aperture AB magnitude	mag
344	SC_IA738_MAGERR_APER2	SC_IA738 2 arcsec diameter aperture AB magnitude error	mag
345	SC_IA738_MAG_APER3	SC_IA738 3 arcsec diameter aperture AB magnitude	mag

346	SC_IA738_MAGERR_APER3	SC_IA738 3 arcsec diameter aperture AB magnitude error	mag
347	SC_IA738_MAG_AUTO	SC_IA738 AUTO AB magnitude	mag
348	SC_IA738_MAGERR_AUTO	SC_IA738 AUTO AB magnitude error	mag
349	SC_IA738_MAG_ISO	SC_IA738 ISO AB magnitude	mag
350	SC_IA738_MAGERR_ISO	SC_IA738 ISO AB magnitude error	mag
351	SC_IA738_FLAGS	SC_IA738 Source Extractor internal flags	
352	SC_IA738_IMAFLAGS_ISO	SC_IA738 flags: 4 means saturated pixel(s) in the isophotal area	
353	SC_IA767_FLUX_APER2	SC_IA767 2 arcsec diameter aperture flux density	uJy
354	SC_IA767_FLUXERR_APER2	SC_IA767 2 arcsec diameter aperture flux density error	uJy
355	SC_IA767_FLUX_APER3	SC_IA767 3 arcsec diameter aperture flux density	uJy
356	SC_IA767_FLUXERR_APER3	SC_IA767 3 arcsec diameter aperture flux density error	uJy
357	SC_IA767_FLUX_AUTO	SC_IA767 AUTO flux density	uJy
358	SC_IA767_FLUXERR_AUTO	SC_IA767 AUTO flux density error	uJy
359	SC_IA767_MAG_APER2	SC_IA767 2 arcsec diameter aperture AB magnitude	mag
360	SC_IA767_MAGERR_APER2	SC_IA767 2 arcsec diameter aperture AB magnitude error	mag
361	SC_IA767_MAG_APER3	SC_IA767 3 arcsec diameter aperture AB magnitude	mag
362	SC_IA767_MAGERR_APER3	SC_IA767 3 arcsec diameter aperture AB magnitude error	mag
363	SC_IA767_MAG_AUTO	SC_IA767 AUTO AB magnitude	mag
364	SC_IA767_MAGERR_AUTO	SC_IA767 AUTO AB magnitude error	mag
365	SC_IA767_MAG_ISO	SC_IA767 ISO AB magnitude	mag
366	SC_IA767_MAGERR_ISO	SC_IA767 ISO AB magnitude error	mag
367	SC_IA767_FLAGS	SC_IA767 Source Extractor internal flags	
368	SC_IA767_IMAFLAGS_ISO	SC_IA767 flags: 4 means saturated pixel(s) in the isophotal area	
369	SC_IB827_FLUX_APER2	SC_IB827 2 arcsec diameter aperture flux density	uJy
370	SC_IB827_FLUXERR_APER2	SC_IB827 2 arcsec diameter aperture flux density error	uJy
371	SC_IB827_FLUX_APER3	SC_IB827 3 arcsec diameter aperture flux density	uJy
372	SC_IB827_FLUXERR_APER3	SC_IB827 3 arcsec diameter aperture flux density error	uJy
373	SC_IB827_FLUX_AUTO	SC_IB827 AUTO flux density	uJy
374	SC_IB827_FLUXERR_AUTO	SC_IB827 AUTO flux density error	uJy
375	SC_IB827_MAG_APER2	SC_IB827 2 arcsec diameter aperture AB magnitude	mag
376	SC_IB827_MAGERR_APER2	SC_IB827 2 arcsec diameter aperture AB magnitude error	mag
377	SC_IB827_MAG_APER3	SC_IB827 3 arcsec diameter aperture AB magnitude	mag
378	SC_IB827_MAGERR_APER3	SC_IB827 3 arcsec diameter aperture AB magnitude error	mag
379	SC_IB827_MAG_AUTO	SC_IB827 AUTO AB magnitude	mag
380	SC_IB827_MAGERR_AUTO	SC_IB827 AUTO AB magnitude error	mag
381	SC_IB827_MAG_ISO	SC_IB827 ISO AB magnitude	mag
382	SC_IB827_MAGERR_ISO	SC_IB827 ISO AB magnitude error	mag
383	SC_IB827_FLAGS	SC_IB827 Source Extractor internal flags	
384	SC_IB827_IMAFLAGS_ISO	SC_IB827 flags: 4 means saturated pixel(s) in the isophotal area	
385	SC_NB711_FLUX_APER2	SC_NB711 2 arcsec diameter aperture flux density	uJy
386	SC_NB711_FLUXERR_APER2	SC_NB711 2 arcsec diameter aperture flux density error	uJy
387	SC_NB711_FLUX_APER3	SC_NB711 3 arcsec diameter aperture flux density	uJy
388	SC_NB711_FLUXERR_APER3	SC_NB711 3 arcsec diameter aperture flux density error	uJy
389	SC_NB711_FLUX_AUTO	SC_NB711 AUTO flux density	uJy
390	SC_NB711_FLUXERR_AUTO	SC_NB711 AUTO flux density error	uJy
391	SC_NB711_MAG_APER2	SC_NB711 2 arcsec diameter aperture AB magnitude	mag
392	SC_NB711_MAGERR_APER2	SC_NB711 2 arcsec diameter aperture AB magnitude error	mag
393	SC_NB711_MAG_APER3	SC_NB711 3 arcsec diameter aperture AB magnitude	mag
394	SC_NB711_MAGERR_APER3	SC_NB711 3 arcsec diameter aperture AB magnitude error	mag
395	SC_NB711_MAG_AUTO	SC_NB711 AUTO AB magnitude	mag
396	SC_NB711_MAGERR_AUTO	SC_NB711 AUTO AB magnitude error	mag
397	SC_NB711_MAG_ISO	SC_NB711 ISO AB magnitude	mag
398	SC_NB711_MAGERR_ISO	SC_NB711 ISO AB magnitude error	mag
399	SC_NB711_FLAGS	SC_NB711 Source Extractor internal flags	
400	SC_NB711_IMAFLAGS_ISO	SC_NB711 flags: 4 means saturated pixel(s) in the isophotal area	
401	SC_NB816_FLUX_APER2	SC_NB816 2 arcsec diameter aperture flux density	uJy
402	SC_NB816_FLUXERR_APER2	SC_NB816 2 arcsec diameter aperture flux density error	uJy
403	SC_NB816_FLUX_APER3	SC_NB816 3 arcsec diameter aperture flux density	uJy
404	SC_NB816_FLUXERR_APER3	SC_NB816 3 arcsec diameter aperture flux density error	uJy
405	SC_NB816_FLUX_AUTO	SC_NB816 AUTO flux density	uJy
406	SC_NB816_FLUXERR_AUTO	SC_NB816 AUTO flux density error	uJy
407	SC_NB816_MAG_APER2	SC_NB816 2 arcsec diameter aperture AB magnitude	mag
408	SC_NB816_MAGERR_APER2	SC_NB816 2 arcsec diameter aperture AB magnitude error	mag
409	SC_NB816_MAG_APER3	SC_NB816 3 arcsec diameter aperture AB magnitude	mag
410	SC_NB816_MAGERR_APER3	SC_NB816 3 arcsec diameter aperture AB magnitude error	mag

411	SC_NB816_MAG_AUTO	SC_NB816 AUTO AB magnitude	mag
412	SC_NB816_MAGERR_AUTO	SC_NB816 AUTO AB magnitude error	mag
413	SC_NB816_MAG_ISO	SC_NB816 ISO AB magnitude	mag
414	SC_NB816_MAGERR_ISO	SC_NB816 ISO AB magnitude error	mag
415	SC_NB816_FLAGS	SC_NB816 Source Extractor internal flags	
416	SC_NB816_IMAFLAGS_ISO	SC_NB816 flags: 4 means saturated pixel(s) in the isophotal area	
417	UVISTA_NB118_FLUX_APER2	UVISTA_NB118 2 arcsec diameter aperture flux density	uJy
418	UVISTA_NB118_FLUXERR_APER2	UVISTA_NB118 2 arcsec diameter aperture flux density error	uJy
419	UVISTA_NB118_FLUX_APER3	UVISTA_NB118 3 arcsec diameter aperture flux density	uJy
420	UVISTA_NB118_FLUXERR_APER3	UVISTA_NB118 3 arcsec diameter aperture flux density error	uJy
421	UVISTA_NB118_FLUX_AUTO	UVISTA_NB118 AUTO flux density	uJy
422	UVISTA_NB118_FLUXERR_AUTO	UVISTA_NB118 AUTO flux density error	uJy
423	UVISTA_NB118_MAG_APER2	UVISTA_NB118 2 arcsec diameter aperture AB magnitude	mag
424	UVISTA_NB118_MAGERR_APER2	UVISTA_NB118 2 arcsec diameter aperture AB magnitude error	mag
425	UVISTA_NB118_MAG_APER3	UVISTA_NB118 3 arcsec diameter aperture AB magnitude	mag
426	UVISTA_NB118_MAGERR_APER3	UVISTA_NB118 3 arcsec diameter aperture AB magnitude error	mag
427	UVISTA_NB118_MAG_AUTO	UVISTA_NB118 AUTO AB magnitude	mag
428	UVISTA_NB118_MAGERR_AUTO	UVISTA_NB118 AUTO AB magnitude error	mag
429	UVISTA_NB118_MAG_ISO	UVISTA_NB118 ISO AB magnitude	mag
430	UVISTA_NB118_MAGERR_ISO	UVISTA_NB118 ISO AB magnitude error	mag
431	UVISTA_NB118_FLAGS	UVISTA_NB118 Source Extractor internal flags	
432	UVISTA_NB118_IMAFLAGS_ISO	UVISTA_NB118 flags: 4 means saturated pixel(s) in the isophotal area	
433	SC_B_FLUX_APER2	SC_B 2 arcsec diameter aperture flux density	uJy
434	SC_B_FLUXERR_APER2	SC_B 2 arcsec diameter aperture flux density error	uJy
435	SC_B_FLUX_APER3	SC_B 3 arcsec diameter aperture flux density	uJy
436	SC_B_FLUXERR_APER3	SC_B 3 arcsec diameter aperture flux density error	uJy
437	SC_B_FLUX_AUTO	SC_B AUTO flux density	uJy
438	SC_B_FLUXERR_AUTO	SC_B AUTO flux density error	uJy
439	SC_B_MAG_APER2	SC_B 2 arcsec diameter aperture AB magnitude	mag
440	SC_B_MAGERR_APER2	SC_B 2 arcsec diameter aperture AB magnitude error	mag
441	SC_B_MAG_APER3	SC_B 3 arcsec diameter aperture AB magnitude	mag
442	SC_B_MAGERR_APER3	SC_B 3 arcsec diameter aperture AB magnitude error	mag
443	SC_B_MAG_AUTO	SC_B AUTO AB magnitude	mag
444	SC_B_MAGERR_AUTO	SC_B AUTO AB magnitude error	mag
445	SC_B_MAG_ISO	SC_B ISO AB magnitude	mag
446	SC_B_MAGERR_ISO	SC_B ISO AB magnitude error	mag
447	SC_B_FLAGS	SC_B Source Extractor internal flags	
448	SC_B_IMAFLAGS_ISO	SC_B flags: 4 means saturated pixel(s) in the isophotal area	
449	SC_gp_FLUX_APER2	SC_gp 2 arcsec diameter aperture flux density	uJy
450	SC_gp_FLUXERR_APER2	SC_gp 2 arcsec diameter aperture flux density error	uJy
451	SC_gp_FLUX_APER3	SC_gp 3 arcsec diameter aperture flux density	uJy
452	SC_gp_FLUXERR_APER3	SC_gp 3 arcsec diameter aperture flux density error	uJy
453	SC_gp_FLUX_AUTO	SC_gp AUTO flux density	uJy
454	SC_gp_FLUXERR_AUTO	SC_gp AUTO flux density error	uJy
455	SC_gp_MAG_APER2	SC_gp 2 arcsec diameter aperture AB magnitude	mag
456	SC_gp_MAGERR_APER2	SC_gp 2 arcsec diameter aperture AB magnitude error	mag
457	SC_gp_MAG_APER3	SC_gp 3 arcsec diameter aperture AB magnitude	mag
458	SC_gp_MAGERR_APER3	SC_gp 3 arcsec diameter aperture AB magnitude error	mag
459	SC_gp_MAG_AUTO	SC_gp AUTO AB magnitude	mag
460	SC_gp_MAGERR_AUTO	SC_gp AUTO AB magnitude error	mag
461	SC_gp_MAG_ISO	SC_gp ISO AB magnitude	mag
462	SC_gp_MAGERR_ISO	SC_gp ISO AB magnitude error	mag
463	SC_gp_FLAGS	SC_gp Source Extractor internal flags	
464	SC_gp_IMAFLAGS_ISO	SC_gp flags: 4 means saturated pixel(s) in the isophotal area	
465	SC_V_FLUX_APER2	SC_V 2 arcsec diameter aperture flux density	uJy
466	SC_V_FLUXERR_APER2	SC_V 2 arcsec diameter aperture flux density error	uJy
467	SC_V_FLUX_APER3	SC_V 3 arcsec diameter aperture flux density	uJy
468	SC_V_FLUXERR_APER3	SC_V 3 arcsec diameter aperture flux density error	uJy
469	SC_V_FLUX_AUTO	SC_V AUTO flux density	uJy
470	SC_V_FLUXERR_AUTO	SC_V AUTO flux density error	uJy
471	SC_V_MAG_APER2	SC_V 2 arcsec diameter aperture AB magnitude	mag
472	SC_V_MAGERR_APER2	SC_V 2 arcsec diameter aperture AB magnitude error	mag
473	SC_V_MAG_APER3	SC_V 3 arcsec diameter aperture AB magnitude	mag
474	SC_V_MAGERR_APER3	SC_V 3 arcsec diameter aperture AB magnitude error	mag
475	SC_V_MAG_AUTO	SC_V AUTO AB magnitude	mag

476	SC_V_MAGERR_AUTO	SC_V AUTO AB magnitude error	mag
477	SC_V_MAG_ISO	SC_V ISO AB magnitude	mag
478	SC_V_MAGERR_ISO	SC_V ISO AB magnitude error	mag
479	SC_V_FLAGS	SC_V Source Extractor internal flags	
480	SC_V_IMAFLAGS_ISO	SC_V flags: 4 means saturated pixel(s) in the isophotal area	
481	SC_rp_FLUX_APER2	SC_rp 2 arcsec diameter aperture flux density	uJy
482	SC_rp_FLUXERR_APER2	SC_rp 2 arcsec diameter aperture flux density error	uJy
483	SC_rp_FLUX_APER3	SC_rp 3 arcsec diameter aperture flux density	uJy
484	SC_rp_FLUXERR_APER3	SC_rp 3 arcsec diameter aperture flux density error	uJy
485	SC_rp_FLUX_AUTO	SC_rp AUTO flux density	uJy
486	SC_rp_FLUXERR_AUTO	SC_rp AUTO flux density error	uJy
487	SC_rp_MAG_APER2	SC_rp 2 arcsec diameter aperture AB magnitude	mag
488	SC_rp_MAGERR_APER2	SC_rp 2 arcsec diameter aperture AB magnitude error	mag
489	SC_rp_MAG_APER3	SC_rp 3 arcsec diameter aperture AB magnitude	mag
490	SC_rp_MAGERR_APER3	SC_rp 3 arcsec diameter aperture AB magnitude error	mag
491	SC_rp_MAG_AUTO	SC_rp AUTO AB magnitude	mag
492	SC_rp_MAGERR_AUTO	SC_rp AUTO AB magnitude error	mag
493	SC_rp_MAG_ISO	SC_rp ISO AB magnitude	mag
494	SC_rp_MAGERR_ISO	SC_rp ISO AB magnitude error	mag
495	SC_rp_FLAGS	SC_rp Source Extractor internal flags	
496	SC_rp_IMAFLAGS_ISO	SC_rp flags: 4 means saturated pixel(s) in the isophotal area	
497	SC_ip_FLUX_APER2	SC_ip 2 arcsec diameter aperture flux density	uJy
498	SC_ip_FLUXERR_APER2	SC_ip 2 arcsec diameter aperture flux density error	uJy
499	SC_ip_FLUX_APER3	SC_ip 3 arcsec diameter aperture flux density	uJy
500	SC_ip_FLUXERR_APER3	SC_ip 3 arcsec diameter aperture flux density error	uJy
501	SC_ip_FLUX_AUTO	SC_ip AUTO flux density	uJy
502	SC_ip_FLUXERR_AUTO	SC_ip AUTO flux density error	uJy
503	SC_ip_MAG_APER2	SC_ip 2 arcsec diameter aperture AB magnitude	mag
504	SC_ip_MAGERR_APER2	SC_ip 2 arcsec diameter aperture AB magnitude error	mag
505	SC_ip_MAG_APER3	SC_ip 3 arcsec diameter aperture AB magnitude	mag
506	SC_ip_MAGERR_APER3	SC_ip 3 arcsec diameter aperture AB magnitude error	mag
507	SC_ip_MAG_AUTO	SC_ip AUTO AB magnitude	mag
508	SC_ip_MAGERR_AUTO	SC_ip AUTO AB magnitude error	mag
509	SC_ip_MAG_ISO	SC_ip ISO AB magnitude	mag
510	SC_ip_MAGERR_ISO	SC_ip ISO AB magnitude error	mag
511	SC_ip_FLAGS	SC_ip Source Extractor internal flags	
512	SC_ip_IMAFLAGS_ISO	SC_ip flags: 4 means saturated pixel(s) in the isophotal area	
513	SC_zp_FLUX_APER2	SC_zp 2 arcsec diameter aperture flux density	uJy
514	SC_zp_FLUXERR_APER2	SC_zp 2 arcsec diameter aperture flux density error	uJy
515	SC_zp_FLUX_APER3	SC_zp 3 arcsec diameter aperture flux density	uJy
516	SC_zp_FLUXERR_APER3	SC_zp 3 arcsec diameter aperture flux density error	uJy
517	SC_zp_FLUX_AUTO	SC_zp AUTO flux density	uJy
518	SC_zp_FLUXERR_AUTO	SC_zp AUTO flux density error	uJy
519	SC_zp_MAG_APER2	SC_zp 2 arcsec diameter aperture AB magnitude	mag
520	SC_zp_MAGERR_APER2	SC_zp 2 arcsec diameter aperture AB magnitude error	mag
521	SC_zp_MAG_APER3	SC_zp 3 arcsec diameter aperture AB magnitude	mag
522	SC_zp_MAGERR_APER3	SC_zp 3 arcsec diameter aperture AB magnitude error	mag
523	SC_zp_MAG_AUTO	SC_zp AUTO AB magnitude	mag
524	SC_zp_MAGERR_AUTO	SC_zp AUTO AB magnitude error	mag
525	SC_zp_MAG_ISO	SC_zp ISO AB magnitude	mag
526	SC_zp_MAGERR_ISO	SC_zp ISO AB magnitude error	mag
527	SC_zp_FLAGS	SC_zp Source Extractor internal flags	
528	SC_zp_IMAFLAGS_ISO	SC_zp flags: 4 means saturated pixel(s) in the isophotal area	
529	SC_zpp_FLUX_APER2	SC_zpp 2 arcsec diameter aperture flux density	uJy
530	SC_zpp_FLUXERR_APER2	SC_zpp 2 arcsec diameter aperture flux density error	uJy
531	SC_zpp_FLUX_APER3	SC_zpp 3 arcsec diameter aperture flux density	uJy
532	SC_zpp_FLUXERR_APER3	SC_zpp 3 arcsec diameter aperture flux density error	uJy
533	SC_zpp_FLUX_AUTO	SC_zpp AUTO flux density	uJy
534	SC_zpp_FLUXERR_AUTO	SC_zpp AUTO flux density error	uJy
535	SC_zpp_MAG_APER2	SC_zpp 2 arcsec diameter aperture AB magnitude	mag
536	SC_zpp_MAGERR_APER2	SC_zpp 2 arcsec diameter aperture AB magnitude error	mag
537	SC_zpp_MAG_APER3	SC_zpp 3 arcsec diameter aperture AB magnitude	mag
538	SC_zpp_MAGERR_APER3	SC_zpp 3 arcsec diameter aperture AB magnitude error	mag
539	SC_zpp_MAG_AUTO	SC_zpp AUTO AB magnitude	mag
540	SC_zpp_MAGERR_AUTO	SC_zpp AUTO AB magnitude error	mag

541	SC_zpp_MAG_ISO	SC_zpp ISO AB magnitude	mag
542	SC_zpp_MAGERR_ISO	SC_zpp ISO AB magnitude error	mag
543	SC_zpp_FLAGS	SC_zpp Source Extractor internal flags	
544	SC_zpp_IMAFLAGS_ISO	SC_zpp flags: 4 means saturated pixel(s) in the isophotal area	
545	total_off2	Aperture-to-total magnitude correction for 2" ap. mags, to be added	mag
546	total_off3	Aperture-to-total magnitude correction for 3" ap. mags, to be added	mag
547	IRAC_CH1_FLUX	IRAC_CH1 flux density	uJy
548	IRAC_CH1_FLUXERR	IRAC_CH1 flux density error	uJy
549	IRAC_CH1_MAG	IRAC_CH1 AB magnitude	mag
550	IRAC_CH1_MAGERR	IRAC_CH1 AB magnitude error	mag
551	IRAC_CH2_FLUX	IRAC_CH2 flux density	uJy
552	IRAC_CH2_FLUXERR	IRAC_CH2 flux density error	uJy
553	IRAC_CH2_MAG	IRAC_CH2 AB magnitude	mag
554	IRAC_CH2_MAGERR	IRAC_CH2 AB magnitude error	mag
555	ID_GALEX	ID in GALEX cat. (Zamojski+2007, Capak+2007), crossm. with 0.6" rad.	
556	GALEX_FUV_FLUX	GALEX_FUV flux density	uJy
557	GALEX_FUV_FLUXERR	GALEX_FUV flux density error	uJy
558	GALEX_FUV_MAG	GALEX_FUV AB magnitude	mag
559	GALEX_FUV_MAGERR	GALEX_FUV AB magnitude error	mag
560	GALEX_NUV_FLUX	GALEX_NUV flux density	uJy
561	GALEX_NUV_FLUXERR	GALEX_NUV flux density error	uJy
562	GALEX_NUV_MAG	GALEX_NUV AB magnitude	mag
563	GALEX_NUV_MAGERR	GALEX_NUV AB magnitude error	mag
564	ID_COSMOS2015	ID in COSMOS2015 cat. (Laigle+2016), crossmatched with 0.6" radius	
565	SPLASH_CH1_FLUX	SPLASH_CH1 flux density	uJy
566	SPLASH_CH1_FLUXERR	SPLASH_CH1 flux density error	uJy
567	SPLASH_CH1_MAG	SPLASH_CH1 AB magnitude	mag
568	SPLASH_CH1_MAGERR	SPLASH_CH1 AB magnitude error	mag
569	SPLASH_CH2_FLUX	SPLASH_CH2 flux density	uJy
570	SPLASH_CH2_FLUXERR	SPLASH_CH2 flux density error	uJy
571	SPLASH_CH2_MAG	SPLASH_CH2 AB magnitude	mag
572	SPLASH_CH2_MAGERR	SPLASH_CH2 AB magnitude error	mag
573	SPLASH_CH3_FLUX	SPLASH_CH3 flux density	uJy
574	SPLASH_CH3_FLUXERR	SPLASH_CH3 flux density error	uJy
575	SPLASH_CH3_MAG	SPLASH_CH3 AB magnitude	mag
576	SPLASH_CH3_MAGERR	SPLASH_CH3 AB magnitude error	mag
577	SPLASH_CH4_FLUX	SPLASH_CH4 flux density	uJy
578	SPLASH_CH4_FLUXERR	SPLASH_CH4 flux density error	uJy
579	SPLASH_CH4_MAG	SPLASH_CH4 AB magnitude	mag
580	SPLASH_CH4_MAGERR	SPLASH_CH4 AB magnitude error	mag
581	ID_ACS	ID in HST ACS F814W cat. (Leauthaud+2007), crossm. with 0.6" radius	
582	ACS_F814W_FLUX	ACS_F814W flux density	uJy
583	ACS_F814W_FLUXERR	ACS_F814W flux density error	uJy
584	ACS_F814W_MAG	ACS_F814W AB magnitude	mag
585	ACS_F814W_MAGERR	ACS_F814W AB magnitude error	mag
586	ACS_A_WORLD	ACS F814W semi-major axis length	deg
587	ACS_B_WORLD	ACS F814W semi-minor axis length	deg
588	ACS_THETA_WORLD	ACS F814W angle; to get PA measured from N through E, add/subtr. 90	deg
589	ACS_FWHM_WORLD	ACS F814W FWHM assuming a gaussian core	deg
590	ACS_MU_MAX	ACS F814W peak surface brightness above background	mag
591	ACS_MU_CLASS	ACS F814W star/galaxy classifier: 1=galaxy, 2=star, 3=fake detection	
592	ID_CHANDRA	ID in Chandra cat. (Civano+2016, Marchesi+2016), crossm. w. 0.6" rad	
593	ID_FARMER	ID in the Farmer catalogue, crossmatched with 0.6" radius	
594	lp_zBEST	LePhare photo-z (=lp_zPDF if galaxy, NaN if X-ray source or masked)	
595	lp_type	LePhare type (0: galaxy, 1: star, 2: Xray sour., -9: failure in fit)	
596	lp_zPDF	LePhare photo-z using the galaxy templ., median of likelihood distr.	
597	lp_zPDF_l68	LePhare photo-z lower limit, 68% confidence level (galaxy templates)	
598	lp_zPDF_u68	LePhare photo-z upper limit, 68% confidence level (galaxy templates)	
599	lp_zMinChi2	LePhare photo-z using the galaxy templates, minimum chi2	
600	lp_chi2_best	LePhare reduced chi2 for lp_zMinChi2 (NaN if less than 3 filters)	
601	lp_zp_2	LePhare 2nd photo-z solution if a 2nd peak detected w. P>5% in PDF	
602	lp_chi2_2	LePhare reduced chi2 for the second photo-z solution	
603	lp_NbFilt	LePhare number of filters used in the fit	
604	lp_zq	LePhare photo-z for the AGN library	
605	lp_chiq	LePhare reduced chi2 for photo-z for the AGN library	

lp_modq	LePhare best fit template number in the AGN library		
lp_mods	LePhare best fit template number in the star library		
lp_chis	LePhare reduced chi2 for the best fit with the star library		
lp_mask	LePhare mask flag (0: in UVISTA and in clean part of HSC and SUPCAM)		
lp_model	LePhare BC03 best fit template number		
lp_age	LePhare BC03 age of best fit template at zPDF	yr	
lp_dust	LePhare BC03 colour excess E(B-V) of best fit template at zPDF		
lp_Attenuation	LePhare BC03 best-fit dust law number at zPDF		
lp_MFUV	LePhare BC03 absolute rest-frame AB mag in GALEX FUV band at zPDF	mag	
lp_MNUV	LePhare BC03 absolute rest-frame AB mag in GALEX NUV band at zPDF	mag	
lp_MU	LePhare BC03 absolute rest-frame AB mag in CFHT u* band at zPDF	mag	
lp_MG	LePhare BC03 absolute rest-frame AB mag in Subaru/HSC g band at zPDF	mag	
lp_MR	LePhare BC03 absolute rest-frame AB mag in Subaru/HSC r band at zPDF	mag	
lp_MI	LePhare BC03 absolute rest-frame AB mag in Subaru/HSC i band at zPDF	mag	
lp_MZ	LePhare BC03 absolute rest-frame AB mag in Subaru/HSC z band at zPDF	mag	
lp_MY	LePhare BC03 absolute rest-frame AB mag in VISTA Y band at zPDF	mag	
lp_MJ	LePhare BC03 absolute rest-frame AB mag in VISTA J band at zPDF	mag	
lp_MH	LePhare BC03 absolute rest-frame AB mag in VISTA H band at zPDF	mag	
lp_MK	LePhare BC03 absolute rest-frame AB mag in VISTA Ks band at zPDF	mag	
lp_mass_med	LePhare BC03 log stellar mass at zPDF	log(solMass)	
lp_mass_med_min68	LePhare BC03 log stellar mass at zPDF, lower limit, 68% conf. level	log(solMass)	
lp_mass_med_max68	LePhare BC03 log stellar mass at zPDF, upper limit, 68% conf. level	log(solMass)	
lp_mass_best	LePhare BC03 log stellar mass at zMinChi2	log(solMass)	
lp_SFR_med	LePhare BC03 log SFR at zPDF	log(solMass/yr)	
lp_SFR_med_min68	LePhare BC03 log SFR at zPDF, lower limit, 68% confidence level	log(solMass/yr)	
lp_SFR_med_max68	LePhare BC03 log SFR at zPDF, upper limit, 68% confidence level	log(solMass/yr)	
lp_SFR_best	LePhare BC03 log SFR at zMinChi2	log(solMass/yr)	
lp_sSFR_med	LePhare BC03 log sSFR at zPDF	log(yr**(-1))	
lp_sSFR_med_min68	LePhare BC03 log sSFR at zPDF, lower limit, 68% confidence level	log(yr**(-1))	
lp_sSFR_med_max68	LePhare BC03 log sSFR at zPDF, upper limit, 68% confidence level	log(yr**(-1))	
lp_sSFR_best	LePhare BC03 log sSFR at zMinChi2	log(yr**(-1))	
ez_z_phot	EAZY maximum a-posteriori photo-z		
ez_z_phot_chi2	EAZY chi2 at ez_z_phot, with z-prior		
ez_z_phot_risk	EAZY risk parameter (Tanaka+2018) at ez_z_phot, R(ez_z_phot)		
ez_z_min_risk	EAZY photo-z where risk parameter R(z) is minimised		
ez_min_risk	EAZY risk parameter at ez_z_min_risk, R(ez_z_min_risk)		
ez_z_raw_chi2	EAZY photo-z where chi2 is minimised, without priors		
ez_raw_chi2	EAZY chi2 at ez_z_raw_chi2		
ez_z025	EAZY 2.5% percentile of photo-z		
ez_z160	EAZY 16.0% percentile of photo-z		
ez_z500	EAZY 50.0% percentile of photo-z		
ez_z840	EAZY 84.0% percentile of photo-z		
ez_z975	EAZY 97.5% percentile of photo-z		
ez_nusefilt	EAZY no. of filters used for photo-z (only filters w/o missing data)		
ez_lc_min	EAZY minimum effective wavelength of valid filters	Angstrom	
ez_lc_max	EAZY minimum effective wavelength of valid filters	Angstrom	
ez_star_min_chi2	EAZY chi2 best stellar template fit (BT-SETTL models) as, 8% sys unc		
ez_star_teff	EAZY effective temperature of the stellar template	K	
ez_restU	EAZY rest-frame U-band flux density	uJy	
ez_restU_err	EAZY rest-frame U-band flux density uncertainty	uJy	
ez_restB	EAZY rest-frame B-band flux density	uJy	
ez_restB_err	EAZY rest-frame B-band flux density uncertainty	uJy	
ez_restV	EAZY rest-frame V-band flux density	uJy	
ez_restV_err	EAZY rest-frame V-band flux density uncertainty	uJy	
ez_restJ	EAZY rest-frame J-band flux density	uJy	
ez_restJ_err	EAZY rest-frame J-band flux density uncertainty	uJy	
ez_dL	EAZY luminosity distance at ez_z_phot	Mpc	
ez_mass	EAZY log stellar mass	log(solMass)	
ez_sfr	EAZY log SFR	log(solMass/yr)	
ez_ssfr	EAZY log sSFR	log(yr**(-1))	
ez_Lv	EAZY log V-band luminosity	log(solLum)	
ez_LIR	EAZY total 8-1000 um luminosity	solLum	
ez_energy_abs	EAZY implied absorbed energy associated with Av	solLum	
ez_Lu	EAZY luminosity in rest-frame U band	solLum	
ez_Lj	EAZY luminosity in rest-frame J band	solLum	

671 | ez_L1400 | EAZY luminosity in tophat filter at 1400 A (200 A wide) rest-frame | solLum
672 | ez_L2800 | EAZY luminosity in tophat filter at 2800 A (200 A wide) rest-frame | solLum
673 | ez_LHa | EAZY Halpha line luminosity (reddened) | solLum
674 | ez_LOIII | EAZY [OIII] 4959+5007 line luminosity (reddened) | solLum
675 | ez_LHb | EAZY Hbeta line luminosity (reddened) | solLum
676 | ez_LOII | EAZY [OII] 3726+3729 line luminosity (reddened) | solLum
677 | ez_MLv | EAZY mass-to-light ratio in V band | solMass/solLum
678 | ez_Av | EAZY extinction in V band | mag
679 | ez_lwAgeV | EAZY light-weighted age in the V band | Gyr
680 | ez_mass_p025 | EAZY 2.5% percentile of log stellar mass | log(solMass)
681 | ez_mass_p160 | EAZY 16.0% percentile of log stellar mass | log(solMass)
682 | ez_mass_p500 | EAZY 50.0% percentile of log stellar mass | log(solMass)
683 | ez_mass_p840 | EAZY 84.0% percentile of log stellar mass | log(solMass)
684 | ez_mass_p975 | EAZY 97.5% percentile of log stellar mass | log(solMass)
685 | ez_sfr_p025 | EAZY 2.5% percentile of log SFR | log(solMass/yr)
686 | ez_sfr_p160 | EAZY 16.0% percentile of log SFR | log(solMass/yr)
687 | ez_sfr_p500 | EAZY 50.0% percentile of log SFR | log(solMass/yr)
688 | ez_sfr_p840 | EAZY 84.0% percentile of log SFR | log(solMass/yr)
689 | ez_sfr_p975 | EAZY 97.5% percentile of log SFR | log(solMass/yr)
690 | ez_Lv_p025 | EAZY 2.5% percentile of log V-band luminosity | log(solLum)
691 | ez_Lv_p160 | EAZY 16.0% percentile of log V-band luminosity | log(solLum)
692 | ez_Lv_p500 | EAZY 50.0% percentile of log V-band luminosity | log(solLum)
693 | ez_Lv_p840 | EAZY 84.0% percentile of log V-band luminosity | log(solLum)
694 | ez_Lv_p975 | EAZY 97.5% percentile of log V-band luminosity | log(solLum)
695 | ez_LIR_p025 | EAZY 2.5% percentile of total 8-1000 um luminosity | solLum
696 | ez_LIR_p160 | EAZY 16.0% percentile of total 8-1000 um luminosity | solLum
697 | ez_LIR_p500 | EAZY 50.0% percentile of total 8-1000 um luminosity | solLum
698 | ez_LIR_p840 | EAZY 84.0% percentile of total 8-1000 um luminosity | solLum
699 | ez_LIR_p975 | EAZY 97.5% percentile of total 8-1000 um luminosity | solLum
700 | ez_energy_abs_p025 | EAZY 2.5% percentile of implied absorbed energy associated with Av | solLum
701 | ez_energy_abs_p160 | EAZY 16.0% percentile of implied absorbed energy associated with Av | solLum
702 | ez_energy_abs_p500 | EAZY 50.0% percentile of implied absorbed energy associated with Av | solLum
703 | ez_energy_abs_p840 | EAZY 84.0% percentile of implied absorbed energy associated with Av | solLum
704 | ez_energy_abs_p975 | EAZY 97.5% percentile of implied absorbed energy associated with Av | solLum
705 | ez_Lu_p025 | EAZY 2.5% percentile of luminosity in rest-frame U band | solLum
706 | ez_Lu_p160 | EAZY 16.0% percentile of luminosity in rest-frame U band | solLum
707 | ez_Lu_p500 | EAZY 50.0% percentile of luminosity in rest-frame U band | solLum
708 | ez_Lu_p840 | EAZY 84.0% percentile of luminosity in rest-frame U band | solLum
709 | ez_Lu_p975 | EAZY 97.5% percentile of luminosity in rest-frame U band | solLum
710 | ez_Lj_p025 | EAZY 2.5% percentile of luminosity in rest-frame J band | solLum
711 | ez_Lj_p160 | EAZY 16.0% percentile of luminosity in rest-frame J band | solLum
712 | ez_Lj_p500 | EAZY 50.0% percentile of luminosity in rest-frame J band | solLum
713 | ez_Lj_p840 | EAZY 84.0% percentile of luminosity in rest-frame J band | solLum
714 | ez_Lj_p975 | EAZY 97.5% percentile of luminosity in rest-frame J band | solLum
715 | ez_L1400_p025 | EAZY 2.5% percentile of lum tophat filter at 1400 A (200 A wide) rf | solLum
716 | ez_L1400_p160 | EAZY 16.0% percentile of lum tophat filter at 1400 A (200 A wide) rf | solLum
717 | ez_L1400_p500 | EAZY 50.0% percentile of lum tophat filter at 1400 A (200 A wide) rf | solLum
718 | ez_L1400_p840 | EAZY 84.0% percentile of lum tophat filter at 1400 A (200 A wide) rf | solLum
719 | ez_L1400_p975 | EAZY 97.5% percentile of lum tophat filter at 1400 A (200 A wide) rf | solLum
720 | ez_L2800_p025 | EAZY 2.5% percentile of lum tophat filter at 2800 A (200 A wide) rf | solLum
721 | ez_L2800_p160 | EAZY 16.0% percentile of lum tophat filter at 2800 A (200 A wide) rf | solLum
722 | ez_L2800_p500 | EAZY 50.0% percentile of lum tophat filter at 2800 A (200 A wide) rf | solLum
723 | ez_L2800_p840 | EAZY 84.0% percentile of lum tophat filter at 2800 A (200 A wide) rf | solLum
724 | ez_L2800_p975 | EAZY 97.5% percentile of lum tophat filter at 2800 A (200 A wide) rf | solLum
725 | ez_LHa_p025 | EAZY 2.5% percentile of Halpha line luminosity (reddened) | solLum
726 | ez_LHa_p160 | EAZY 16.0% percentile of Halpha line luminosity (reddened) | solLum
727 | ez_LHa_p500 | EAZY 50.0% percentile of Halpha line luminosity (reddened) | solLum
728 | ez_LHa_p840 | EAZY 84.0% percentile of Halpha line luminosity (reddened) | solLum
729 | ez_LHa_p975 | EAZY 97.5% percentile of Halpha line luminosity (reddened) | solLum
730 | ez_LOIII_p025 | EAZY 2.5% percentile of [OIII] 4959+5007 line luminosity (reddened) | solLum
731 | ez_LOIII_p160 | EAZY 16.0% percentile of [OIII] 4959+5007 line luminosity (reddened) | solLum
732 | ez_LOIII_p500 | EAZY 50.0% percentile of [OIII] 4959+5007 line luminosity (reddened) | solLum
733 | ez_LOIII_p840 | EAZY 84.0% percentile of [OIII] 4959+5007 line luminosity (reddened) | solLum
734 | ez_LOIII_p975 | EAZY 97.5% percentile of [OIII] 4959+5007 line luminosity (reddened) | solLum
735 | ez_LHb_p025 | EAZY 2.5% percentile of Hbeta line luminosity (reddened) | solLum

736	ez_LHb_p160	EAZY 16.0% percentile of Hbeta line luminosity (reddened)	solLum
737	ez_LHb_p500	EAZY 50.0% percentile of Hbeta line luminosity (reddened)	solLum
738	ez_LHb_p840	EAZY 84.0% percentile of Hbeta line luminosity (reddened)	solLum
739	ez_LHb_p975	EAZY 97.5% percentile of Hbeta line luminosity (reddened)	solLum
740	ez_LOII_p025	EAZY 2.5% percentile of [OII] 3726+3729 line luminosity (reddened)	solLum
741	ez_LOII_p160	EAZY 16.0% percentile of [OII] 3726+3729 line luminosity (reddened)	solLum
742	ez_LOII_p500	EAZY 50.0% percentile of [OII] 3726+3729 line luminosity (reddened)	solLum
743	ez_LOII_p840	EAZY 84.0% percentile of [OII] 3726+3729 line luminosity (reddened)	solLum
744	ez_LOII_p975	EAZY 97.5% percentile of [OII] 3726+3729 line luminosity (reddened)	solLum
745	ez_ssfr_p025	EAZY 2.5% percentile of log sSFR	log(yr**(-1))
746	ez_ssfr_p160	EAZY 16.0% percentile of log sSFR	log(yr**(-1))
747	ez_ssfr_p500	EAZY 50.0% percentile of log sSFR	log(yr**(-1))
748	ez_ssfr_p840	EAZY 84.0% percentile of log sSFR	log(yr**(-1))
749	ez_ssfr_p975	EAZY 97.5% percentile of log sSFR	log(yr**(-1))
750	ez_Av_p025	EAZY 2.5% percentile of extinction in V band	mag
751	ez_Av_p160	EAZY 16.0% percentile of extinction in V band	mag
752	ez_Av_p500	EAZY 50.0% percentile of extinction in V band	mag
753	ez_Av_p840	EAZY 84.0% percentile of extinction in V band	mag
754	ez_Av_p975	EAZY 97.5% percentile of extinction in V band	mag

6.2 Complete list of The Farmer catalogue columns

The following is a list of number, name, description and unit for all the columns in The Farmer.

No.	Column name	Column description	Column unit
1	ID	ID (specifically ID_FARMER, as this is the Farmer catalogue)	
2	ALPHA_J2000	Right ascension (J2000) of model, or of SEP when model is not avail.	deg
3	DELTA_J2000	Declination (J2000) of model, or of SEP when model is not available	deg
4	X_MODEL	Object model position along X, with the scale being 0.15"/px	pix
5	Y_MODEL	Object model position along Y, with the scale being 0.15"/px	pix
6	ERRX_MODEL	Uncertainty on object model position along X	pix
7	ERRY_MODEL	Uncertainty on object model position along Y	pix
8	ALPHA_DETECTION	Right ascension (J2000) of object as determined by SEP at detection	deg
9	DELTA_DETECTION	Declination (J2000) of object as determined by SEP at detection	deg
10	FARMER_ID	Farmer internal source identifier ({brick}_{source})	
11	GROUP_ID	Farmer group identifier; unique within a brick	
12	N_GROUP	Farmer group occupation number	
13	MODEL_FLAG	Flag (0: OK, 1: failed to converge, 2: drifted >0.6" from detection)	
14	SOLUTION_MODEL	The Tractor model type selected by The Farmer	
15	FLAG_HSC	Flag indicating quality of HSC imaging (0:clean, 1:masked)	
16	FLAG_SUPCAM	Flag indicating quality of Suprime-Cam imaging (0:clean, 1:masked)	
17	FLAG_UDEEP	Flag for the UltraVISTA ultra-deep regions (0:ultra-deep, 1:deep)	
18	FLAG_UVISTA	Flag for the UltraVISTA region (0:inside, 1:outside)	
19	FLAG_COMBINED	Comb. FLAG_UVISTA, FLAG_HSC, FLAG_SUPCAM (0:clean and inside UVISTA)	
20	EBV_MW	Galactic reddening E(B-V) (Schlegel+1998, Schlafly&Finkbeiner 2011)	
21	CFHT_u_FLUX	CFHT_u flux density	uJy
22	CFHT_u_FLUXERR	CFHT_u flux density error	uJy
23	CFHT_u_MAG	CFHT_u AB magnitude	mag
24	CFHT_u_MAGERR	CFHT_u AB magnitude error	mag
25	CFHT_u_CHISQ	CFHT_u reduced Chi2 goodness of fit stat for source prof model	
26	CFHT_u_DRIFT	CFHT_u distance travelled from RA,Dec model centroid	arcsec
27	CFHT_u_VALID	CFHT_u flag=False if FLUX/MAG or its error is not trustworthy	
28	CFHT_ustar_FLUX	CFHT_ustar flux density	uJy
29	CFHT_ustar_FLUXERR	CFHT_ustar flux density error	uJy
30	CFHT_ustar_MAG	CFHT_ustar AB magnitude	mag
31	CFHT_ustar_MAGERR	CFHT_ustar AB magnitude error	mag
32	CFHT_ustar_CHISQ	CFHT_ustar reduced Chi2 goodness of fit stat for source prof model	
33	CFHT_ustar_DRIFT	CFHT_ustar distance travelled from RA,Dec model centroid	arcsec
34	CFHT_ustar_VALID	CFHT_ustar flag=False if FLUX/MAG or its error is not trustworthy	
35	HSC_g_FLUX	HSC_g flux density	uJy
36	HSC_g_FLUXERR	HSC_g flux density error	uJy
37	HSC_g_MAG	HSC_g AB magnitude	mag

38	HSC_g_MAGERR	HSC_g AB magnitude error	mag
39	HSC_g_CHISQ	HSC_g reduced Chi2 goodness of fit stat for source prof model	
40	HSC_g_DRIFT	HSC_g distance travelled from RA,Dec model centroid	arcsec
41	HSC_g_VALID	HSC_g flag=False if FLUX/MAG or its error is not trustworthy	
42	HSC_r_FLUX	HSC_r flux density	uJy
43	HSC_r_FLUXERR	HSC_r flux density error	uJy
44	HSC_r_MAG	HSC_r AB magnitude	mag
45	HSC_r_MAGERR	HSC_r AB magnitude error	mag
46	HSC_r_CHISQ	HSC_r reduced Chi2 goodness of fit stat for source prof model	
47	HSC_r_DRIFT	HSC_r distance travelled from RA,Dec model centroid	arcsec
48	HSC_r_VALID	HSC_r flag=False if FLUX/MAG or its error is not trustworthy	
49	HSC_i_FLUX	HSC_i flux density	uJy
50	HSC_i_FLUXERR	HSC_i flux density error	uJy
51	HSC_i_MAG	HSC_i AB magnitude	mag
52	HSC_i_MAGERR	HSC_i AB magnitude error	mag
53	HSC_i_CHISQ	HSC_i reduced Chi2 goodness of fit stat for source prof model	
54	HSC_i_DRIFT	HSC_i distance travelled from RA,Dec model centroid	arcsec
55	HSC_i_VALID	HSC_i flag=False if FLUX/MAG or its error is not trustworthy	
56	HSC_z_FLUX	HSC_z flux density	uJy
57	HSC_z_FLUXERR	HSC_z flux density error	uJy
58	HSC_z_MAG	HSC_z AB magnitude	mag
59	HSC_z_MAGERR	HSC_z AB magnitude error	mag
60	HSC_z_CHISQ	HSC_z reduced Chi2 goodness of fit stat for source prof model	
61	HSC_z_DRIFT	HSC_z distance travelled from RA,Dec model centroid	arcsec
62	HSC_z_VALID	HSC_z flag=False if FLUX/MAG or its error is not trustworthy	
63	HSC_y_FLUX	HSC_y flux density	uJy
64	HSC_y_FLUXERR	HSC_y flux density error	uJy
65	HSC_y_MAG	HSC_y AB magnitude	mag
66	HSC_y_MAGERR	HSC_y AB magnitude error	mag
67	HSC_y_CHISQ	HSC_y reduced Chi2 goodness of fit stat for source prof model	
68	HSC_y_DRIFT	HSC_y distance travelled from RA,Dec model centroid	arcsec
69	HSC_y_VALID	HSC_y flag=False if FLUX/MAG or its error is not trustworthy	
70	UVISTA_Y_FLUX	UVISTA_Y flux density	uJy
71	UVISTA_Y_FLUXERR	UVISTA_Y flux density error	uJy
72	UVISTA_Y_MAG	UVISTA_Y AB magnitude	mag
73	UVISTA_Y_MAGERR	UVISTA_Y AB magnitude error	mag
74	UVISTA_Y_CHISQ	UVISTA_Y reduced Chi2 goodness of fit stat for source prof model	
75	UVISTA_Y_DRIFT	UVISTA_Y distance travelled from RA,Dec model centroid	arcsec
76	UVISTA_Y_VALID	UVISTA_Y flag=False if FLUX/MAG or its error is not trustworthy	
77	UVISTA_J_FLUX	UVISTA_J flux density	uJy
78	UVISTA_J_FLUXERR	UVISTA_J flux density error	uJy
79	UVISTA_J_MAG	UVISTA_J AB magnitude	mag
80	UVISTA_J_MAGERR	UVISTA_J AB magnitude error	mag
81	UVISTA_J_CHISQ	UVISTA_J reduced Chi2 goodness of fit stat for source prof model	
82	UVISTA_J_DRIFT	UVISTA_J distance travelled from RA,Dec model centroid	arcsec
83	UVISTA_J_VALID	UVISTA_J flag=False if FLUX/MAG or its error is not trustworthy	
84	UVISTA_H_FLUX	UVISTA_H flux density	uJy
85	UVISTA_H_FLUXERR	UVISTA_H flux density error	uJy
86	UVISTA_H_MAG	UVISTA_H AB magnitude	mag
87	UVISTA_H_MAGERR	UVISTA_H AB magnitude error	mag
88	UVISTA_H_CHISQ	UVISTA_H reduced Chi2 goodness of fit stat for source prof model	
89	UVISTA_H_DRIFT	UVISTA_H distance travelled from RA,Dec model centroid	arcsec
90	UVISTA_H_VALID	UVISTA_H flag=False if FLUX/MAG or its error is not trustworthy	
91	UVISTA_Ks_FLUX	UVISTA_Ks flux density	uJy
92	UVISTA_Ks_FLUXERR	UVISTA_Ks flux density error	uJy
93	UVISTA_Ks_MAG	UVISTA_Ks AB magnitude	mag
94	UVISTA_Ks_MAGERR	UVISTA_Ks AB magnitude error	mag
95	UVISTA_Ks_CHISQ	UVISTA_Ks reduced Chi2 goodness of fit stat for source prof model	
96	UVISTA_Ks_DRIFT	UVISTA_Ks distance travelled from RA,Dec model centroid	arcsec
97	UVISTA_Ks_VALID	UVISTA_Ks flag=False if FLUX/MAG or its error is not trustworthy	
98	UVISTA_NB118_FLUX	UVISTA_NB118 flux density	uJy
99	UVISTA_NB118_FLUXERR	UVISTA_NB118 flux density error	uJy
100	UVISTA_NB118_MAG	UVISTA_NB118 AB magnitude	mag
101	UVISTA_NB118_MAGERR	UVISTA_NB118 AB magnitude error	mag
102	UVISTA_NB118_CHISQ	UVISTA_NB118 reduced Chi2 goodness of fit stat for source prof model	

103	UVISTA_NB118_DRIFT	UVISTA_NB118 distance travelled from RA,Dec model centroid	arcsec
104	UVISTA_NB118_VALID	UVISTA_NB118 flag=False if FLUX/MAG or its error is not trustworthy	
105	SC_IB427_FLUX	SC_IB427 flux density	uJy
106	SC_IB427_FLUXERR	SC_IB427 flux density error	uJy
107	SC_IB427_MAG	SC_IB427 AB magnitude	mag
108	SC_IB427_MAGERR	SC_IB427 AB magnitude error	mag
109	SC_IB427_CHISQ	SC_IB427 reduced Chi2 goodness of fit stat for source prof model	
110	SC_IB427_DRIFT	SC_IB427 distance travelled from RA,Dec model centroid	arcsec
111	SC_IB427_VALID	SC_IB427 flag=False if FLUX/MAG or its error is not trustworthy	
112	SC_IB464_FLUX	SC_IB464 flux density	uJy
113	SC_IB464_FLUXERR	SC_IB464 flux density error	uJy
114	SC_IB464_MAG	SC_IB464 AB magnitude	mag
115	SC_IB464_MAGERR	SC_IB464 AB magnitude error	mag
116	SC_IB464_CHISQ	SC_IB464 reduced Chi2 goodness of fit stat for source prof model	
117	SC_IB464_DRIFT	SC_IB464 distance travelled from RA,Dec model centroid	arcsec
118	SC_IB464_VALID	SC_IB464 flag=False if FLUX/MAG or its error is not trustworthy	
119	SC_IA484_FLUX	SC_IA484 flux density	uJy
120	SC_IA484_FLUXERR	SC_IA484 flux density error	uJy
121	SC_IA484_MAG	SC_IA484 AB magnitude	mag
122	SC_IA484_MAGERR	SC_IA484 AB magnitude error	mag
123	SC_IA484_CHISQ	SC_IA484 reduced Chi2 goodness of fit stat for source prof model	
124	SC_IA484_DRIFT	SC_IA484 distance travelled from RA,Dec model centroid	arcsec
125	SC_IA484_VALID	SC_IA484 flag=False if FLUX/MAG or its error is not trustworthy	
126	SC_IB505_FLUX	SC_IB505 flux density	uJy
127	SC_IB505_FLUXERR	SC_IB505 flux density error	uJy
128	SC_IB505_MAG	SC_IB505 AB magnitude	mag
129	SC_IB505_MAGERR	SC_IB505 AB magnitude error	mag
130	SC_IB505_CHISQ	SC_IB505 reduced Chi2 goodness of fit stat for source prof model	
131	SC_IB505_DRIFT	SC_IB505 distance travelled from RA,Dec model centroid	arcsec
132	SC_IB505_VALID	SC_IB505 flag=False if FLUX/MAG or its error is not trustworthy	
133	SC_IA527_FLUX	SC_IA527 flux density	uJy
134	SC_IA527_FLUXERR	SC_IA527 flux density error	uJy
135	SC_IA527_MAG	SC_IA527 AB magnitude	mag
136	SC_IA527_MAGERR	SC_IA527 AB magnitude error	mag
137	SC_IA527_CHISQ	SC_IA527 reduced Chi2 goodness of fit stat for source prof model	
138	SC_IA527_DRIFT	SC_IA527 distance travelled from RA,Dec model centroid	arcsec
139	SC_IA527_VALID	SC_IA527 flag=False if FLUX/MAG or its error is not trustworthy	
140	SC_IB574_FLUX	SC_IB574 flux density	uJy
141	SC_IB574_FLUXERR	SC_IB574 flux density error	uJy
142	SC_IB574_MAG	SC_IB574 AB magnitude	mag
143	SC_IB574_MAGERR	SC_IB574 AB magnitude error	mag
144	SC_IB574_CHISQ	SC_IB574 reduced Chi2 goodness of fit stat for source prof model	
145	SC_IB574_DRIFT	SC_IB574 distance travelled from RA,Dec model centroid	arcsec
146	SC_IB574_VALID	SC_IB574 flag=False if FLUX/MAG or its error is not trustworthy	
147	SC_IA624_FLUX	SC_IA624 flux density	uJy
148	SC_IA624_FLUXERR	SC_IA624 flux density error	uJy
149	SC_IA624_MAG	SC_IA624 AB magnitude	mag
150	SC_IA624_MAGERR	SC_IA624 AB magnitude error	mag
151	SC_IA624_CHISQ	SC_IA624 reduced Chi2 goodness of fit stat for source prof model	
152	SC_IA624_DRIFT	SC_IA624 distance travelled from RA,Dec model centroid	arcsec
153	SC_IA624_VALID	SC_IA624 flag=False if FLUX/MAG or its error is not trustworthy	
154	SC_IA679_FLUX	SC_IA679 flux density	uJy
155	SC_IA679_FLUXERR	SC_IA679 flux density error	uJy
156	SC_IA679_MAG	SC_IA679 AB magnitude	mag
157	SC_IA679_MAGERR	SC_IA679 AB magnitude error	mag
158	SC_IA679_CHISQ	SC_IA679 reduced Chi2 goodness of fit stat for source prof model	
159	SC_IA679_DRIFT	SC_IA679 distance travelled from RA,Dec model centroid	arcsec
160	SC_IA679_VALID	SC_IA679 flag=False if FLUX/MAG or its error is not trustworthy	
161	SC_IB709_FLUX	SC_IB709 flux density	uJy
162	SC_IB709_FLUXERR	SC_IB709 flux density error	uJy
163	SC_IB709_MAG	SC_IB709 AB magnitude	mag
164	SC_IB709_MAGERR	SC_IB709 AB magnitude error	mag
165	SC_IB709_CHISQ	SC_IB709 reduced Chi2 goodness of fit stat for source prof model	
166	SC_IB709_DRIFT	SC_IB709 distance travelled from RA,Dec model centroid	arcsec
167	SC_IB709_VALID	SC_IB709 flag=False if FLUX/MAG or its error is not trustworthy	

```
168 | SC_IA738_FLUX        | SC_IA738 flux density                                                | uJy
169 | SC_IA738_FLUXERR     | SC_IA738 flux density error                                          | uJy
170 | SC_IA738_MAG         | SC_IA738 AB magnitude                                                | mag
171 | SC_IA738_MAGERR      | SC_IA738 AB magnitude error                                          | mag
172 | SC_IA738_CHISQ       | SC_IA738 reduced Chi2 goodness of fit stat for source prof model     |
173 | SC_IA738_DRIFT       | SC_IA738 distance travelled from RA,Dec model centroid               | arcsec
174 | SC_IA738_VALID       | SC_IA738 flag=False if FLUX/MAG or its error is not trustworthy      |
175 | SC_IA767_FLUX        | SC_IA767 flux density                                                | uJy
176 | SC_IA767_FLUXERR     | SC_IA767 flux density error                                          | uJy
177 | SC_IA767_MAG         | SC_IA767 AB magnitude                                                | mag
178 | SC_IA767_MAGERR      | SC_IA767 AB magnitude error                                          | mag
179 | SC_IA767_CHISQ       | SC_IA767 reduced Chi2 goodness of fit stat for source prof model     |
180 | SC_IA767_DRIFT       | SC_IA767 distance travelled from RA,Dec model centroid               | arcsec
181 | SC_IA767_VALID       | SC_IA767 flag=False if FLUX/MAG or its error is not trustworthy      |
182 | SC_IB827_FLUX        | SC_IB827 flux density                                                | uJy
183 | SC_IB827_FLUXERR     | SC_IB827 flux density error                                          | uJy
184 | SC_IB827_MAG         | SC_IB827 AB magnitude                                                | mag
185 | SC_IB827_MAGERR      | SC_IB827 AB magnitude error                                          | mag
186 | SC_IB827_CHISQ       | SC_IB827 reduced Chi2 goodness of fit stat for source prof model     |
187 | SC_IB827_DRIFT       | SC_IB827 distance travelled from RA,Dec model centroid               | arcsec
188 | SC_IB827_VALID       | SC_IB827 flag=False if FLUX/MAG or its error is not trustworthy      |
189 | SC_NB711_FLUX        | SC_NB711 flux density                                                | uJy
190 | SC_NB711_FLUXERR     | SC_NB711 flux density error                                          | uJy
191 | SC_NB711_MAG         | SC_NB711 AB magnitude                                                | mag
192 | SC_NB711_MAGERR      | SC_NB711 AB magnitude error                                          | mag
193 | SC_NB711_CHISQ       | SC_NB711 reduced Chi2 goodness of fit stat for source prof model     |
194 | SC_NB711_DRIFT       | SC_NB711 distance travelled from RA,Dec model centroid               | arcsec
195 | SC_NB711_VALID       | SC_NB711 flag=False if FLUX/MAG or its error is not trustworthy      |
196 | SC_NB816_FLUX        | SC_NB816 flux density                                                | uJy
197 | SC_NB816_FLUXERR     | SC_NB816 flux density error                                          | uJy
198 | SC_NB816_MAG         | SC_NB816 AB magnitude                                                | mag
199 | SC_NB816_MAGERR      | SC_NB816 AB magnitude error                                          | mag
200 | SC_NB816_CHISQ       | SC_NB816 reduced Chi2 goodness of fit stat for source prof model     |
201 | SC_NB816_DRIFT       | SC_NB816 distance travelled from RA,Dec model centroid               | arcsec
202 | SC_NB816_VALID       | SC_NB816 flag=False if FLUX/MAG or its error is not trustworthy      |
203 | IRAC_CH1_FLUX        | IRAC_CH1 flux density                                                | uJy
204 | IRAC_CH1_FLUXERR     | IRAC_CH1 flux density error                                          | uJy
205 | IRAC_CH1_MAG         | IRAC_CH1 AB magnitude                                                | mag
206 | IRAC_CH1_MAGERR      | IRAC_CH1 AB magnitude error                                          | mag
207 | IRAC_CH1_CHISQ       | IRAC_CH1 reduced Chi2 goodness of fit stat for source prof model     |
208 | IRAC_CH1_DRIFT       | IRAC_CH1 distance travelled from RA,Dec model centroid               | arcsec
209 | IRAC_CH1_VALID       | IRAC_CH1 flag=False if FLUX/MAG or its error is not trustworthy      |
210 | IRAC_CH2_FLUX        | IRAC_CH2 flux density                                                | uJy
211 | IRAC_CH2_FLUXERR     | IRAC_CH2 flux density error                                          | uJy
212 | IRAC_CH2_MAG         | IRAC_CH2 AB magnitude                                                | mag
213 | IRAC_CH2_MAGERR      | IRAC_CH2 AB magnitude error                                          | mag
214 | IRAC_CH2_CHISQ       | IRAC_CH2 reduced Chi2 goodness of fit stat for source prof model     |
215 | IRAC_CH2_DRIFT       | IRAC_CH2 distance travelled from RA,Dec model centroid               | arcsec
216 | IRAC_CH2_VALID       | IRAC_CH2 flag=False if FLUX/MAG or its error is not trustworthy      |
217 | IRAC_CH3_FLUX        | IRAC_CH3 flux density                                                | uJy
218 | IRAC_CH3_FLUXERR     | IRAC_CH3 flux density error                                          | uJy
219 | IRAC_CH3_MAG         | IRAC_CH3 AB magnitude                                                | mag
220 | IRAC_CH3_MAGERR      | IRAC_CH3 AB magnitude error                                          | mag
221 | IRAC_CH3_CHISQ       | IRAC_CH3 reduced Chi2 goodness of fit stat for source prof model     |
222 | IRAC_CH3_DRIFT       | IRAC_CH3 distance travelled from RA,Dec model centroid               | arcsec
223 | IRAC_CH3_VALID       | IRAC_CH3 flag=False if FLUX/MAG or its error is not trustworthy      |
224 | IRAC_CH4_FLUX        | IRAC_CH4 flux density                                                | uJy
225 | IRAC_CH4_FLUXERR     | IRAC_CH4 flux density error                                          | uJy
226 | IRAC_CH4_MAG         | IRAC_CH4 AB magnitude                                                | mag
227 | IRAC_CH4_MAGERR      | IRAC_CH4 AB magnitude error                                          | mag
228 | IRAC_CH4_CHISQ       | IRAC_CH4 reduced Chi2 goodness of fit stat for source prof model     |
229 | IRAC_CH4_DRIFT       | IRAC_CH4 distance travelled from RA,Dec model centroid               | arcsec
230 | IRAC_CH4_VALID       | IRAC_CH4 flag=False if FLUX/MAG or its error is not trustworthy      |
231 | ID_GALEX             | ID in GALEX cat. (Zamojski+2007, Capak+2007), crossm. with 0.6" rad. |
232 | GALEX_NUV_FLUX       | GALEX_NUV flux density                                               | uJy
```

233	GALEX_NUV_FLUXERR	GALEX_NUV flux density error	uJy
234	GALEX_NUV_MAG	GALEX_NUV AB magnitude	mag
235	GALEX_NUV_MAGERR	GALEX_NUV AB magnitude error	mag
236	GALEX_FUV_FLUX	GALEX_FUV flux density	uJy
237	GALEX_FUV_FLUXERR	GALEX_FUV flux density error	uJy
238	GALEX_FUV_MAG	GALEX_FUV AB magnitude	mag
239	GALEX_FUV_MAGERR	GALEX_FUV AB magnitude error	mag
240	ID_COSMOS2015	ID in COSMOS2015 cat. (Laigle+2016), crossmatched with 0.6" radius	
241	SPLASH_CH1_FLUX	SPLASH_CH1 flux density	uJy
242	SPLASH_CH1_FLUXERR	SPLASH_CH1 flux density error	uJy
243	SPLASH_CH1_MAG	SPLASH_CH1 AB magnitude	mag
244	SPLASH_CH1_MAGERR	SPLASH_CH1 AB magnitude error	mag
245	SPLASH_CH2_FLUX	SPLASH_CH2 flux density	uJy
246	SPLASH_CH2_FLUXERR	SPLASH_CH2 flux density error	uJy
247	SPLASH_CH2_MAG	SPLASH_CH2 AB magnitude	mag
248	SPLASH_CH2_MAGERR	SPLASH_CH2 AB magnitude error	mag
249	SPLASH_CH3_FLUX	SPLASH_CH3 flux density	uJy
250	SPLASH_CH3_FLUXERR	SPLASH_CH3 flux density error	uJy
251	SPLASH_CH3_MAG	SPLASH_CH3 AB magnitude	mag
252	SPLASH_CH3_MAGERR	SPLASH_CH3 AB magnitude error	mag
253	SPLASH_CH4_FLUX	SPLASH_CH4 flux density	uJy
254	SPLASH_CH4_FLUXERR	SPLASH_CH4 flux density error	uJy
255	SPLASH_CH4_MAG	SPLASH_CH4 AB magnitude	mag
256	SPLASH_CH4_MAGERR	SPLASH_CH4 AB magnitude error	mag
257	ID_ACS	ID in HST ACS F814W cat. (Leauthaud+2007), crossm. with 0.6" radius	
258	ACS_F814W_MAG	ACS_F814W AB magnitude	mag
259	ACS_F814W_MAGERR	ACS_F814W AB magnitude error	mag
260	ACS_F814W_FLUX	ACS_F814W flux density	uJy
261	ACS_F814W_FLUXERR	ACS_F814W flux density error	uJy
262	ACS_A_WORLD	ACS F814W semi-major axis length	deg
263	ACS_B_WORLD	ACS F814W semi-minor axis length	deg
264	ACS_THETA_WORLD	ACS F814W angle; to get PA measured from N through E, add/subtr. 90	deg
265	ACS_FWHM_WORLD	ACS F814W FWHM assuming a gaussian core	deg
266	ACS_MU_MAX	ACS F814W peak surface brightness above background	
267	ACS_MU_CLASS	ACS F814W star/galaxy classifier: 1=galaxy, 2=star, 3=fake detection	
268	ID_CHANDRA	ID in Chandra cat. (Civano+2016, Marchesi+2016), crossm. w. 0.6" rad	
269	ID_CLASSIC	ID in the Classic catalogue, crossmatched with 0.6" radius	
270	lp_zBEST	LePhare photo-z (=lp_zPDF if galaxy, NaN if X-ray source or masked)	
271	lp_type	LePhare type (0: galaxy, 1: star, 2: Xray sour., -9: failure in fit)	
272	lp_zPDF	LePhare photo-z using the galaxy templ., median of likelihood distr.	
273	lp_zPDF_l68	LePhare photo-z lower limit, 68% confidence level (galaxy templates)	
274	lp_zPDF_u68	LePhare photo-z upper limit, 68% confidence level (galaxy templates)	
275	lp_zMinChi2	LePhare photo-z using the galaxy templates, minimum chi2	
276	lp_chi2_best	LePhare reduced chi2 for lp_zMinChi2 (NaN if less than 3 filters)	
277	lp_zp_2	LePhare 2nd photo-z solution if a 2nd peak detected w. P>5% in PDF	
278	lp_chi2_2	LePhare reduced chi2 for the second photo-z solution	
279	lp_NbFilt	LePhare number of filters used in the fit	
280	lp_zq	LePhare photo-z for the AGN library	
281	lp_chiq	LePhare reduced chi2 for photo-z for the AGN library	
282	lp_modq	LePhare best fit template number in the AGN library	
283	lp_mods	LePhare best fit template number in the star library	
284	lp_chis	LePhare reduced chi2 for the best fit with the star library	
285	lp_mask	LePhare mask flag (0: in UVISTA and in clean part of HSC and SUPCAM)	
286	lp_model	LePhare BC03 best fit template number	
287	lp_age	LePhare BC03 age of best fit template at zPDF	yr
288	lp_dust	LePhare BC03 colour excess E(B-V) of best fit template at zPDF	
289	lp_Attenuation	LePhare BC03 best-fit dust law number at zPDF	
290	lp_MFUV	LePhare BC03 absolute rest-frame AB mag in GALEX FUV band at zPDF	mag
291	lp_MNUV	LePhare BC03 absolute rest-frame AB mag in GALEX NUV band at zPDF	mag
292	lp_MU	LePhare BC03 absolute rest-frame AB mag in CFHT u* band at zPDF	mag
293	lp_MG	LePhare BC03 absolute rest-frame AB mag in Subaru/HSC g band at zPDF	mag
294	lp_MR	LePhare BC03 absolute rest-frame AB mag in Subaru/HSC r band at zPDF	mag
295	lp_MI	LePhare BC03 absolute rest-frame AB mag in Subaru/HSC i band at zPDF	mag
296	lp_MZ	LePhare BC03 absolute rest-frame AB mag in Subaru/HSC z band at zPDF	mag
297	lp_MY	LePhare BC03 absolute rest-frame AB mag in VISTA Y band at zPDF	mag

298	lp_MJ	LePhare BC03 absolute rest-frame AB mag in VISTA J band at zPDF	mag
299	lp_MH	LePhare BC03 absolute rest-frame AB mag in VISTA H band at zPDF	mag
300	lp_MK	LePhare BC03 absolute rest-frame AB mag in VISTA Ks band at zPDF	mag
301	lp_mass_med	LePhare BC03 log stellar mass at zPDF	log(solMass)
302	lp_mass_med_min68	LePhare BC03 log stellar mass at zPDF, lower limit, 68% conf. level	log(solMass)
303	lp_mass_med_max68	LePhare BC03 log stellar mass at zPDF, upper limit, 68% conf. level	log(solMass)
304	lp_mass_best	LePhare BC03 log stellar mass at zMinChi2	log(solMass)
305	lp_SFR_med	LePhare BC03 log SFR at zPDF	log(solMass/yr)
306	lp_SFR_med_min68	LePhare BC03 log SFR at zPDF, lower limit, 68% confidence level	log(solMass/yr)
307	lp_SFR_med_max68	LePhare BC03 log SFR at zPDF, upper limit, 68% confidence level	log(solMass/yr)
308	lp_SFR_best	LePhare BC03 log SFR at zMinChi2	log(solMass/yr)
309	lp_sSFR_med	LePhare BC03 log sSFR at zPDF	log(yr**(-1))
310	lp_sSFR_med_min68	LePhare BC03 log sSFR at zPDF, lower limit, 68% confidence level	log(yr**(-1))
311	lp_sSFR_med_max68	LePhare BC03 log sSFR at zPDF, upper limit, 68% confidence level	log(yr**(-1))
312	lp_sSFR_best	LePhare BC03 log sSFR at zMinChi2	log(yr**(-1))
313	ez_z_phot	EAZY maximum a-posteriori photo-z	
314	ez_z_phot_chi2	EAZY chi2 at ez_z_phot, with z-prior	
315	ez_z_phot_risk	EAZY risk parameter (Tanaka+2018) at ez_z_phot, R(ez_z_phot)	
316	ez_z_min_risk	EAZY photo-z where risk parameter R(z) is minimised	
317	ez_min_risk	EAZY risk parameter at ez_z_min_risk, R(ez_z_min_risk)	
318	ez_z_raw_chi2	EAZY photo-z where chi2 is minimised, without priors	
319	ez_raw_chi2	EAZY chi2 at ez_z_raw_chi2	
320	ez_z025	EAZY 2.5% percentile of photo-z	
321	ez_z160	EAZY 16.0% percentile of photo-z	
322	ez_z500	EAZY 50.0% percentile of photo-z	
323	ez_z840	EAZY 84.0% percentile of photo-z	
324	ez_z975	EAZY 97.5% percentile of photo-z	
325	ez_nusefilt	EAZY no. of filters used for photo-z (only filters w/o missing data)	
326	ez_lc_min	EAZY minimum effective wavelength of valid filters	Angstrom
327	ez_lc_max	EAZY minimum effective wavelength of valid filters	Angstrom
328	ez_star_min_chi2	EAZY chi2 best stellar template fit (BT-SETTL models) as, 8% sys unc	
329	ez_star_teff	EAZY effective temperature of the stellar template	K
330	ez_restU	EAZY rest-frame U-band flux density	uJy
331	ez_restU_err	EAZY rest-frame U-band flux density uncertainty	uJy
332	ez_restB	EAZY rest-frame B-band flux density	uJy
333	ez_restB_err	EAZY rest-frame B-band flux density uncertainty	uJy
334	ez_restV	EAZY rest-frame V-band flux density	uJy
335	ez_restV_err	EAZY rest-frame V-band flux density uncertainty	uJy
336	ez_restJ	EAZY rest-frame J-band flux density	uJy
337	ez_restJ_err	EAZY rest-frame J-band flux density uncertainty	uJy
338	ez_dL	EAZY luminosity distance at ez_z_phot	Mpc
339	ez_mass	EAZY log stellar mass	log(solMass)
340	ez_sfr	EAZY log SFR	log(solMass/yr)
341	ez_ssfr	EAZY log sSFR	log(yr**(-1))
342	ez_Lv	EAZY log V-band luminosity	log(solLum)
343	ez_LIR	EAZY total 8-1000 um luminosity	solLum
344	ez_energy_abs	EAZY implied absorbed energy associated with Av	solLum
345	ez_Lu	EAZY luminosity in rest-frame U band	solLum
346	ez_Lj	EAZY luminosity in rest-frame J band	solLum
347	ez_L1400	EAZY luminosity in tophat filter at 1400 A (200 A wide) rest-frame	solLum
348	ez_L2800	EAZY luminosity in tophat filter at 2800 A (200 A wide) rest-frame	solLum
349	ez_LHa	EAZY Halpha line luminosity (reddened)	solLum
350	ez_LOIII	EAZY [OIII] 4959+5007 line luminosity (reddened)	solLum
351	ez_LHb	EAZY Hbeta line luminosity (reddened)	solLum
352	ez_LOII	EAZY [OII] 3726+3729 line luminosity (reddened)	solLum
353	ez_MLv	EAZY mass-to-light ratio in V band	solMass/solLum
354	ez_Av	EAZY extinction in V band	mag
355	ez_lwAgeV	EAZY light-weighted age in the V band	Gyr
356	ez_mass_p025	EAZY 2.5% percentile of log stellar mass	log(solMass)
357	ez_mass_p160	EAZY 16.0% percentile of log stellar mass	log(solMass)
358	ez_mass_p500	EAZY 50.0% percentile of log stellar mass	log(solMass)
359	ez_mass_p840	EAZY 84.0% percentile of log stellar mass	log(solMass)
360	ez_mass_p975	EAZY 97.5% percentile of log stellar mass	log(solMass)
361	ez_sfr_p025	EAZY 2.5% percentile of log SFR	log(solMass/yr)
362	ez_sfr_p160	EAZY 16.0% percentile of log SFR	log(solMass/yr)

```
363 | ez_sfr_p500          | EAZY 50.0% percentile of log SFR                                    | log(solMass/yr)
364 | ez_sfr_p840          | EAZY 84.0% percentile of log SFR                                    | log(solMass/yr)
365 | ez_sfr_p975          | EAZY 97.5% percentile of log SFR                                    | log(solMass/yr)
366 | ez_Lv_p025           | EAZY  2.5% percentile of log V-band luminosity                      | log(solLum)
367 | ez_Lv_p160           | EAZY 16.0% percentile of log V-band luminosity                      | log(solLum)
368 | ez_Lv_p500           | EAZY 50.0% percentile of log V-band luminosity                      | log(solLum)
369 | ez_Lv_p840           | EAZY 84.0% percentile of log V-band luminosity                      | log(solLum)
370 | ez_Lv_p975           | EAZY 97.5% percentile of log V-band luminosity                      | log(solLum)
371 | ez_LIR_p025          | EAZY  2.5% percentile of total 8-1000 um luminosity                 | solLum
372 | ez_LIR_p160          | EAZY 16.0% percentile of total 8-1000 um luminosity                 | solLum
373 | ez_LIR_p500          | EAZY 50.0% percentile of total 8-1000 um luminosity                 | solLum
374 | ez_LIR_p840          | EAZY 84.0% percentile of total 8-1000 um luminosity                 | solLum
375 | ez_LIR_p975          | EAZY 97.5% percentile of total 8-1000 um luminosity                 | solLum
376 | ez_energy_abs_p025   | EAZY  2.5% percentile of implied absorbed energy associated with Av | solLum
377 | ez_energy_abs_p160   | EAZY 16.0% percentile of implied absorbed energy associated with Av | solLum
378 | ez_energy_abs_p500   | EAZY 50.0% percentile of implied absorbed energy associated with Av | solLum
379 | ez_energy_abs_p840   | EAZY 84.0% percentile of implied absorbed energy associated with Av | solLum
380 | ez_energy_abs_p975   | EAZY 97.5% percentile of implied absorbed energy associated with Av | solLum
381 | ez_Lu_p025           | EAZY  2.5% percentile of luminosity in rest-frame U band            | solLum
382 | ez_Lu_p160           | EAZY 16.0% percentile of luminosity in rest-frame U band            | solLum
383 | ez_Lu_p500           | EAZY 50.0% percentile of luminosity in rest-frame U band            | solLum
384 | ez_Lu_p840           | EAZY 84.0% percentile of luminosity in rest-frame U band            | solLum
385 | ez_Lu_p975           | EAZY 97.5% percentile of luminosity in rest-frame U band            | solLum
386 | ez_Lj_p025           | EAZY  2.5% percentile of luminosity in rest-frame J band            | solLum
387 | ez_Lj_p160           | EAZY 16.0% percentile of luminosity in rest-frame J band            | solLum
388 | ez_Lj_p500           | EAZY 50.0% percentile of luminosity in rest-frame J band            | solLum
389 | ez_Lj_p840           | EAZY 84.0% percentile of luminosity in rest-frame J band            | solLum
390 | ez_Lj_p975           | EAZY 97.5% percentile of luminosity in rest-frame J band            | solLum
391 | ez_L1400_p025        | EAZY  2.5% percentile of lum tophat filter at 1400 A (200 A wide) rf | solLum
392 | ez_L1400_p160        | EAZY 16.0% percentile of lum tophat filter at 1400 A (200 A wide) rf | solLum
393 | ez_L1400_p500        | EAZY 50.0% percentile of lum tophat filter at 1400 A (200 A wide) rf | solLum
394 | ez_L1400_p840        | EAZY 84.0% percentile of lum tophat filter at 1400 A (200 A wide) rf | solLum
395 | ez_L1400_p975        | EAZY 97.5% percentile of lum tophat filter at 1400 A (200 A wide) rf | solLum
396 | ez_L2800_p025        | EAZY  2.5% percentile of lum tophat filter at 2800 A (200 A wide) rf | solLum
397 | ez_L2800_p160        | EAZY 16.0% percentile of lum tophat filter at 2800 A (200 A wide) rf | solLum
398 | ez_L2800_p500        | EAZY 50.0% percentile of lum tophat filter at 2800 A (200 A wide) rf | solLum
399 | ez_L2800_p840        | EAZY 84.0% percentile of lum tophat filter at 2800 A (200 A wide) rf | solLum
400 | ez_L2800_p975        | EAZY 97.5% percentile of lum tophat filter at 2800 A (200 A wide) rf | solLum
401 | ez_LHa_p025          | EAZY  2.5% percentile of Halpha line luminosity (reddened)          | solLum
402 | ez_LHa_p160          | EAZY 16.0% percentile of Halpha line luminosity (reddened)          | solLum
403 | ez_LHa_p500          | EAZY 50.0% percentile of Halpha line luminosity (reddened)          | solLum
404 | ez_LHa_p840          | EAZY 84.0% percentile of Halpha line luminosity (reddened)          | solLum
405 | ez_LHa_p975          | EAZY 97.5% percentile of Halpha line luminosity (reddened)          | solLum
406 | ez_LOIII_p025        | EAZY  2.5% percentile of [OIII] 4959+5007 line luminosity (reddened) | solLum
407 | ez_LOIII_p160        | EAZY 16.0% percentile of [OIII] 4959+5007 line luminosity (reddened) | solLum
408 | ez_LOIII_p500        | EAZY 50.0% percentile of [OIII] 4959+5007 line luminosity (reddened) | solLum
409 | ez_LOIII_p840        | EAZY 84.0% percentile of [OIII] 4959+5007 line luminosity (reddened) | solLum
410 | ez_LOIII_p975        | EAZY 97.5% percentile of [OIII] 4959+5007 line luminosity (reddened) | solLum
411 | ez_LHb_p025          | EAZY  2.5% percentile of Hbeta line luminosity (reddened)           | solLum
412 | ez_LHb_p160          | EAZY 16.0% percentile of Hbeta line luminosity (reddened)           | solLum
413 | ez_LHb_p500          | EAZY 50.0% percentile of Hbeta line luminosity (reddened)           | solLum
414 | ez_LHb_p840          | EAZY 84.0% percentile of Hbeta line luminosity (reddened)           | solLum
415 | ez_LHb_p975          | EAZY 97.5% percentile of Hbeta line luminosity (reddened)           | solLum
416 | ez_LOII_p025         | EAZY  2.5% percentile of [OII] 3726+3729 line luminosity (reddened) | solLum
417 | ez_LOII_p160         | EAZY 16.0% percentile of [OII] 3726+3729 line luminosity (reddened) | solLum
418 | ez_LOII_p500         | EAZY 50.0% percentile of [OII] 3726+3729 line luminosity (reddened) | solLum
419 | ez_LOII_p840         | EAZY 84.0% percentile of [OII] 3726+3729 line luminosity (reddened) | solLum
420 | ez_LOII_p975         | EAZY 97.5% percentile of [OII] 3726+3729 line luminosity (reddened) | solLum
421 | ez_ssfr_p025         | EAZY  2.5% percentile of log sSFR                                   | log(yr**(-1))
422 | ez_ssfr_p160         | EAZY 16.0% percentile of log sSFR                                   | log(yr**(-1))
423 | ez_ssfr_p500         | EAZY 50.0% percentile of log sSFR                                   | log(yr**(-1))
424 | ez_ssfr_p840         | EAZY 84.0% percentile of log sSFR                                   | log(yr**(-1))
425 | ez_ssfr_p975         | EAZY 97.5% percentile of log sSFR                                   | log(yr**(-1))
426 | ez_Av_p025           | EAZY  2.5% percentile of extinction in V band                       | mag
427 | ez_Av_p160           | EAZY 16.0% percentile of extinction in V band                       | mag
```

```
428 | ez_Av_p500          | EAZY 50.0% percentile of extinction in V band                    | mag
429 | ez_Av_p840          | EAZY 84.0% percentile of extinction in V band                    | mag
430 | ez_Av_p975          | EAZY 97.5% percentile of extinction in V band                    | mag
```

References

Arnouts, S., Moscardini, L., Vanzella, E., et al. 2002, MNRAS, 329, 355

Astropy Collaboration, Price-Whelan, A. M., Sipőcz, B. M., et al. 2018, The Astronomical Journal, 156, 123, aDS Bibcode: 2018AJ....156..123A

Barbary, K. 2016, The Journal of Open Source Software, 1, 58

Bertin, E. & Arnouts, S. 1996, A&AS, 117, 393

Brammer, G. B., van Dokkum, P. G., & Coppi, P. 2008, ApJ, 686, 1503

Drlica-Wagner, A., Sevilla-Noarbe, I., Rykoff, E. S., et al. 2018, ApJS, 235, 33

Gaia Collaboration, Brown, A. G. A., Vallenari, A., et al. 2016, Astronomy & Astrophysics, 595, A2

Gaia Collaboration, Brown, A. G. A., Vallenari, A., et al. 2018, Astronomy & Astrophysics, 616, A1

Hsieh, B.-C., Wang, W.-H., Hsieh, C.-C., et al. 2012, The Astrophysical Journal Supplement Series, 203, 23

Ilbert, O., Arnouts, S., McCracken, H. J., et al. 2006, A&A, 457, 841

Laigle, C., McCracken, H. J., Ilbert, O., et al. 2016, ApJS, 224, 24

Lang, D., Hogg, D. W., & Mykytyn, D. 2016, Astrophysics Source Code Library, ascl:1604.008

McCracken, H. J., Milvang-Jensen, B., Dunlop, J., et al. 2012, Astronomy and Astrophysics, 544, A156

Robitaille, T. P., Tollerud, E. J., Greenfield, P., et al. 2013, Astronomy & Astrophysics, 558, A33, publisher: EDP Sciences

Taylor, M. B. 2006, in Astronomical Society of the Pacific Conference Series, Vol. 351, Astronomical Data Analysis Software and Systems XV, ed. C. Gabriel, C. Arviset, D. Ponz, & S. Enrique, 666

Weaver, J. R., Kauffmann, O. B., Ilbert, O., et al. 2022, ApJS, 258, 11